

6774

6774  
JNCASR  
532.053 P09

JNCASR  
ACC  
NO. --6774  
LIBRARY

# Algebraic Instability and Transient Growth in Stratified Shear Flows

A Thesis

Submitted for the Degree of  
**MASTER OF SCIENCE (ENGINEERING)**  
in the Faculty of Engineering

by  
RAHUL BALE



ENGINEERING MECHANICS UNIT  
JAWAHARLAL NEHRU CENTRE FOR ADVANCED SCIENTIFIC  
RESEARCH  
(A Deemed University)  
Bangalore – 560 064

August 2009

532.053  
p09

*To My Parents*

## DECLARATION

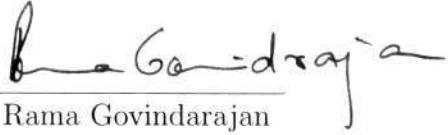
I hereby declare that the matter embodied in the thesis entitled “**Algebraic Instability and Transient Growth in Stratified Shear Flows**” is the result of investigations carried out by me at the Engineering Mechanics Unit, Jawaharlal Nehru Centre for Advanced Scientific Research, Bangalore, India under the supervision of Prof. Rama Govindarajan and that it has not been submitted elsewhere for the award of any degree or diploma.

In keeping with the general practice in reporting scientific observations, due acknowledgment has been made whenever the work described is based on the findings of other investigators.

  
Rahul Bale

## CERTIFICATE

I hereby certify that the matter embodied in this thesis entitled “**Algebraic Instability and Transient Growth in Stratified Shear Flows**” has been carried out by Mr. Rahul Bale at the Engineering Mechanics Unit, Jawaharlal Nehru Centre for Advanced Scientific Research, Bangalore, India under my supervision and that it has not been submitted elsewhere for the award of any degree or diploma.



---

Prof. Rama Govindarajan

(Research Supervisor)

## Acknowledgments

It is worth spending a page out of this thesis to acknowledge and express my gratitude towards the people who made this possible.

Prof. Rama Govindarajan, my thesis adviser, for her guidance and advice in my research. Her never ending enthusiasm towards research and to understand new problems always inspired me to do more. I cannot recall having met any of the deadlines she set for me, yet she always gave me more time which shows the enormous amount of patience she has. For counseling me when I was low on confidence about my abilities to do research.

Anubhab for the numerous pedagogical discussions we had. His knowledge of the literature on various aspects of fluid mechanics is commendable. These were the discussions that led to our collaboration on the stability of stratified shear flows.

Sameen for helping me with the transient growth code and for having discussions and arguments all the way from IIT Madras.

Aditya for his help with the DNS that I tried to develop although I could not use it for my thesis.

Sumesh for always being there to help when anybody needed him.

Tulra for wasting quite a lot of my time with discussions and arguments on random topics ranging from politics to movies to music, although I must admit that I had wonderful time discussing these things.

Punnu for being so naive that it made her a natural *bakra* which made life at room 103 so much fun. Krithika for making me teach her transient growth and stability which helped me brush up my basics and also for being the other *bakra* of room 103.

Vivek Parkas and Anna Bond for being good friends. Harry for taking everything that I and Anubhab did to him sportively. Dabade, Dhiraj, Dinesh, Gayathri, Kopal, Shady Shastry, Srikanth and others for all their help.

The summer students, Veera, Chandra, Miru, Pallavi and many others for making life at JNC more cheerful. Darshan for all his never ending inquisitive questions which made me rethink what I had taken for granted.





# Contents

|   |             |
|---|-------------|
| <b>Abstract</b>   | <b>ix</b>   |
| <b>List of Figures</b>  | <b>xiii</b> |
| <b>1 Nonnormality and Transient Growth</b>                        | <b>3</b>    |
| 1.1 2D system . . . . .   | 3           |
| 1.1.1 Condition for growth . . . . .                              | 4           |
| 1.1.2 Optimal C . . . . .   | 6           |
| 1.2 An initial value problem . . . . .                            | 8           |
| <b>2 Algebraic Instability in Inviscid Stratified Shear Flows</b> | <b>13</b>   |
| 2.1 Introduction . . . . .  | 13          |
| 2.2 Stability of Stratified Shear Flow . . . . .                  | 17          |
| 2.3 An Analogy . . . . .  | 18          |
| 2.4 Transient Growth Mechanism . . . . .                          | 21          |
| 2.5 Algebraic Growth . . . . .                                    | 24          |
| 2.5.1 Toy Problem: Brown and Stewartson(1979) . . . . .           | 25          |
| 2.5.2 Full Inviscid problem . . . . .                             | 32          |
| <b>3 Transient Growth in Viscous Stratified Shear Flow</b>        | <b>37</b>   |
| 3.1 Linear Stability . . . . .                                    | 37          |
| 3.2 Transient Growth . . . . .                                    | 40          |
| 3.3 Couette Flow . . . . .  | 43          |
| 3.3.1 Stable Stratification . . . . .                             | 43          |
| 3.3.2 Unstable Stratification . . . . .                           | 49          |
| 3.4 Poiseuille Flow - Density Stratification . . . . .            | 51          |
| 3.4.1 Stable Stratification . . . . .                             | 51          |

|          |   |           |
|----------|---|-----------|
| 3.4.2    | Unstable Stratification . . . . .                               | 55        |
| 3.5      | Poiseuille Flow: Viscosity and Density Stratification . . . . . | 57        |
| 3.5.1    | Mean velocity profile . . . . .                                 | 57        |
| 3.5.2    | Viscosity Stratification . . . . .                              | 62        |
| 3.5.3    | Viscosity and Density Stratification . . . . .                  | 63        |
| 3.5.4    | Energy Definitoin . . . . .                                     | 67        |
| <b>4</b> | <b>Conclusions and Future Outlook</b>                           | <b>71</b> |
|          | <b>References</b>   | <b>73</b> |

## Abstract

In the present work we study the asymptotic and short time stability of stratified shear flow analytically and numerically. The algebraic growth and instability of stably stratified inviscid Couette flow is studied analytically. A transient growth analysis has been carried out on both stable and unstable stratification for viscous Couette and Poiseuille flow. Stratification in viscosity has also been considered in the study of Poiseuille flow.

To begin with we tried to understand the nonnormality and transient growth through a simple two dimension nonnormal system. With this 2D system we demonstrate that nonnormality is a necessary but not a sufficient condition for transient growth. We derive the limits of nonnormality in which the system can exhibit transient growth. The dependence of transient growth on the initial condition has also been studied and the initial condition which gives the maximum possible growth at a given time is derived.

The stability of stratified Couette flow is a well studied problem in literature, yet the problem is not well understood. The mechanisms by which the flow becomes unstable, e.g. how atmospheric turbulence sets in is still a problem of open research. Traditionally the main interests lay in obtaining the large time exponent for the flow perturbations to make predictions on the stability of the flow. It was not until the 1990's that the transient aspect of the problem was looked at. We have carried out work on the bounded inviscid Couette flow to address both short time as well long time aspect of the stability. To understand and explain the problem we first use a toy problem. We show in the toy problem that there is a linear instability for singular initial condition in temperature and an algebraic growth for smooth initial conditions. The asymptotic exponents we obtain for the full problem are in agreement with the literature. Based on the toy problem we argue for the full problem that there will be transient algebraic growth for a smooth initial condition, although this still has to be numerically verified.

In the viscous analysis we study the effect of stratification on the transient growth. In the density stratified Couette flow we find that a stable stratification decreases the maximum transient growth and an unstable stratification increases it. It was also found that stable stratification increases the spanwise dependence of disturbances causing the maximum transient growth. The results for the Poiseuille are qualitatively similar to the Couette flow case for both stable and unstable stratification. Including viscosity stratification leads to very large transient growth. When density stratification is considered along with viscosity stratification it has very little effect on the transient growth and there is no qualitative change in the nature of transient growth.

## List of Figures

|      |   |    |
|------|---|----|
| 1.1  | Nonnormal vectors and transient growth in the resultant . . . . .   | 4  |
| 1.2  | The maximum transient growth $G_{max}$ as a function of the initial ratio $C$ of the magnitudes of the two vectors. The different lines correspond to various values of the angle $180-\phi$ between the vectors, beginning with $\phi = 0^0$ for the topmost curve, and ending with $\phi = 3.82^0$ for the bottom curve shown by the plus symbols. The values of $\phi$ in between are $0.42^0, 0.85^0, 1.27^0, 1.69^0, 2.12^0, 2.55^0, 2.97^0$ and $3.39^0$ respectively. The bottom curve corresponds to the critical value of $\phi$ , hence smaller angles between the two vectors would ensure a decay of their resultant. . . . . | 7  |
| 1.3  | Evolution of the optimal growth . . . . .   | 10 |
| 1.4  | Linear and nonlinear evolution of normal and nonnormal matrices . . . . .   | 11 |
| 2.1  | Stratification profiles a) with depth in oceans b) with height in the atmosphere (Pedlosky (1986)) . . . . .  | 14 |
| 2.2  | Schematic of stably stratified Couette flow . . . . .   | 15 |
| 2.3  | A brief literature survey . . . . .   | 18 |
| 2.4  | Illustration of the Lift-up effect. Figure courtesy Anubhab Roy . . . . .   | 22 |
| 2.5  | Orr-Mechanism of transient growth in a 2D flow. . . . .   | 23 |
| 2.6  | Temperature perturbations Profiles . . . . .  | 27 |
| 2.7  | Stream function at $t=5$ for a pure thermal perturbation. . . . .   | 28 |
| 2.8  | Stream function at $t=22$ for a pure thermal perturbation. . . . .  | 29 |
| 2.9  | Evolution of energy due to pure vorticity perturbation, i.e. no temperature perturbation . . . . .  | 29 |
| 2.10 | Evolution of energy due to pure temperature perturbation with no vorticity perturbation. . . . .  | 30 |
| 2.11 | Wave Interaction . . . . .  | 30 |

|      |   |    |
|------|---|----|
| 2.12 | Dependence of $t_{max}$ on the width of the Gaussian initial temperature profile. . . . .   | 31 |
| 2.13 | Variation of $E_{max}$ with the width of the Gaussian initial temperature profile. . . . .  | 31 |
| 3.1  | Evolution of $g$ for random initial conditions . . . . .  | 42 |
| 3.2  | $G_{max}$ contours for plane couette flow without stratification. . . . .   | 44 |
| 3.3  | $G_{max}$ contours with stratification, $Gr = 10$ , $Pr = 10^{-4}$ . . . . .  | 46 |
| 3.4  | Same as Fig: 3.3 but $Pr = 10^{-1}$ . . . . .   | 46 |
| 3.5  | Same as Fig: 3.3 but $Pr = 1$ . . . . .   | 47 |
| 3.6  | Increased Richardson number with $Gr = 1000$ & $Pr = 10^{-1}$ . . . . .   | 47 |
| 3.7  | $Gr=10000$ $Pr = 10^{-1}$ . . . . .   | 48 |
| 3.8  | $Gr=10000$ $Pr = 1$ . . . . .   | 48 |
| 3.9  | $Gr = -10$ , $Pr = 0.1$ , Transient growth does not change at small $Gr$ and small $Pr$ . . . . .   | 49 |
| 3.10 | $Gr = -10$ , $Pr = 1$ , Transient growth increase when $Pr$ is increased . . . . .  | 50 |
| 3.11 | There is an increase in transient growth with increase in $Gr$ , $Gr = -1000$ & $Pr = 0.1$ . . . . .  | 50 |
| 3.12 | $G_{max}$ contours of unheated Poiseuille flow . . . . .  | 51 |
| 3.13 | $Gr = 1$ and $Pr = 10^{-3}$ , there is hardly any change in the transient growth from the unheated case. . . . .  | 52 |
| 3.14 | Stably Stratified Poiseuille flow with $Gr = 1$ and $Pr = 1$ . . . . .  | 53 |
| 3.15 | In stable stratification Increasing Buoyancy seems to decrease transient growth, $Gr = 1000$ and $Pr = 1$ . . . . .                                       | 53 |
| 3.16 | The Transient growth is reduced even more with increase in Buoyancy, $Gr = 10000$ and $Pr = 1$ . . . . .  | 54 |
| 3.17 | Unstable stratification with $Gr = -1$ , $Pr = 10^{-3}$ . . . . .   | 54 |
| 3.18 | $Gr = -1$ , $Pr = 1$ , increasing Prandtl number increases transient growth. . . . .  | 55 |
| 3.19 | $Gr = -1$ , $Pr = 10^{-1}$ . . . . .  | 56 |
| 3.20 | Same as Fig: 3.19 but $Gr = -1000$ , increasing Buoyancy increases transient growth. . . . .  | 56 |
| 3.21 | Velocity profile for stratified and unstratified case with different level of stratification. The velocity is normalized by the maximum velocity. . . . . | 57 |

|      |   |    |
|------|---|----|
| 3.22 | Viscosity profile for stratified and unstratified case. The viscosity is normalized by viscosity at the hot wall. . . . . | 58 |
| 3.23 | Variation of first derivative of velocity with $y$ for different level of stratification . . . . .                        | 59 |
| 3.24 | Variation of first derivative of viscosity with $y$ for different level of stratification . . . . .                       | 59 |
| 3.25 | Variation of second derivative of velocity with $y$ for different level of stratification . . . . .                       | 60 |
| 3.26 | Variation of second derivative of viscosity with $y$ for different level of stratification . . . . .                      | 60 |
| 3.27 | Variation of third derivative of velocity with $y$ for different level of stratification . . . . .                        | 61 |
| 3.28 | Variation of third derivative of viscosity with $y$ for different level of stratification . . . . .                       | 61 |
| 3.29 | Only viscosity stratification, $Pr = 10^{-4}$ . . . . .   | 64 |
| 3.30 | increasing $Pr$ increases the transient growth, $Pr = 10^{-1}$ . . . . .  | 64 |
| 3.31 | There is a dramatic increase in the transient growth, $Pr = 1$ . . . . .  | 65 |
| 3.32 | Introducing small density stratification suppresses the growth, $Gr = 100$ and $Pr = 1$ . . . . .                         | 65 |
| 3.33 | $Gr = 10000$ and $Pr = 0.1$ . . . . .   | 66 |
| 3.34 | At large Grashof the reduction in transient growth is much larger, $Gr = 10000$ and $Pr = 1$ . . . . .                    | 66 |
| 3.35 | Effect of the Choice of $B$ on the total energy. with $B = 0.1$ and $Pr = 0.1$ a) $Gr = -10000$ b) $Gr = 1000$ . . . . .  | 67 |
| 3.36 | Same as Fig 3.35, $B = 1$ . . . . .   | 68 |
| 3.37 | Same as Fig 3.35, $B = 10$ . . . . .  | 69 |





## CHAPTER 1

# NONNORMALITY AND TRANSIENT GROWTH

Flow problems are generally very complicated and it is not easy to understand the concept of nonnormality if one directly ventures into addressing flow problems. It is instructive to start with a simple system, a toy model, to understand nonnormality and hence transient growth. In this chapter we consider a simple 2 dimensional system as a toy model to understand how nonnormality leads to transient growth. With this model we examine under what circumstances transient growth occurs. We explore the parameter space to arrive at the maximum possible growth for the system in terms of optimal initial conditions.

### 1.1 2D system

It easy is to imagine nonnormality in a system through the angle between its eigenvectors if the dimensionality of the system is 3 or less. We consider a 2 dimensional system whose eigenvectors are at an angle other than  $\pi/2$ , i.e. the vectors are nonorthogonal or *nonnormal*. In Fig: 1.1 vectors  $\vec{X}_1$  and  $\vec{X}_2$  are shown which are at an angle  $\pi-\phi$ , where  $\phi \neq \pi/2$ . Here  $\vec{X}_1$  and  $\vec{X}_2$  are assumed to be time varying, they can either increase or decrease with time while remaining oriented in their respective directions. The idea of transient growth is relevant to stable systems where short time growth in decaying quantities can be seen, but in an unstable system where quantities are already growing only traces of transient growth can be seen which is usually not of interest. As our interest lies in the growth of some quantity at short times in asymptotically stable systems we consider the case of decaying vectors. As is of the case in linear problems the vectors are taken to be exponentially varying and are given by  $\vec{X}_1 = e^{-\lambda_1 t}$  and  $\vec{X}_2 = Ce^{-\lambda_2 t}$ , where  $\lambda_1, \lambda_2$  are positive real constants.

In physical systems the quantity under scrutiny is the total energy of perturbations to the system, if the energy decays with time then the system is stable, unstable otherwise. Energy in a flow problem is the kinetic energy which is the sum of squares of individual velocities. An analogous definition of energy in the toy model is the square of the resultant of the two vectors. The magnitude of the

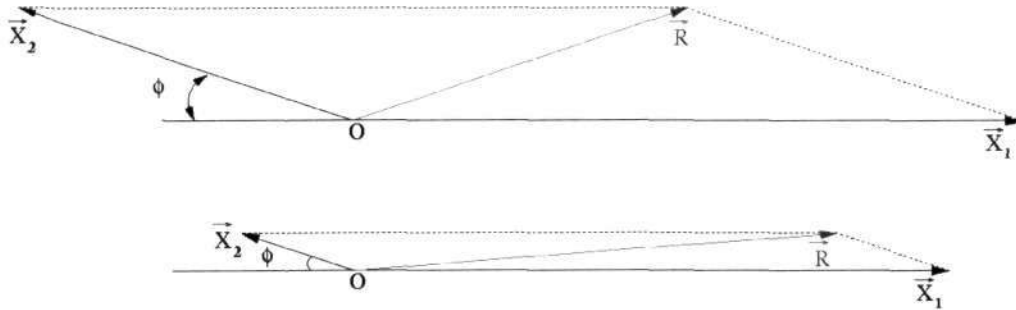


Figure 1.1: Nonnormal vectors and transient growth in the resultant

resultant of the vectors is given by

$$R^2 = (e^{-\lambda_1 t} - C \cos \phi e^{-\lambda_2 t})^2 + (C \sin \phi e^{-\lambda_2 t})^2. \quad (1.1)$$

As the vectors are modeled with decaying exponential it is intuitively expected that the resultant,  $R$ , will also decay with time. The negative exponents give a picture only of the asymptotic behavior of  $R$ , but interestingly at small times a growth in  $R$  can be seen which seems to defy logic. This growth of a quantity at small times in the vicinity of  $t = 0_+$  before eventual decay is called *transient growth*.

### 1.1.1 Condition for growth

A system which is nonnormal may not always exhibit transient growth under any condition, i.e nonnormality is necessary but not sufficient for transient growth. We will see why this is true by the end of this section. For any growth in  $R$  at some time during its evolution the slope of  $R$  with respect to  $t$  must be greater than zero

$$\frac{dR}{dt} > 0. \quad (1.2)$$

For simplicity let us define

$$y = \frac{e^{(\lambda_2 - \lambda_1)t}}{C} = \frac{z}{C} \text{ and } r = \frac{\lambda_2}{\lambda_1}. \quad (1.3)$$

Without loss of generality we can assume  $\lambda_1 > \lambda_2$  so that  $r < 1$ . Using the definition of  $y$  and  $r$ , applying the condition for slope from Eq (1.2) on  $R$  we get an inequality in terms of  $y$

$$y^2 - y(1+r)\cos\phi + r < 0. \quad (1.4)$$

If  $C$  is less than zero then the above inequality cannot be satisfied hence we choose  $C$  greater than zero. For  $C$  greater than zero the solution for the above inequality is given by

$$y < \frac{(1+r)}{2} \left[ \cos\phi \pm \sqrt{\left(\frac{1-r}{1+r}\right)^2 - \sin^2\phi} \right]. \quad (1.5)$$

We have assumed  $\lambda_1, \lambda_2$  to be positive real constants so  $y$  must also be real. Hence for  $y$  to be real,

$$\sin^{-1}\left(\frac{-(1-r)}{1+r}\right) < \phi < \sin^{-1}\left(\frac{1-r}{1+r}\right). \quad (1.6)$$

We now have a condition on  $\phi$  for a given pair of  $\lambda_1, \lambda_2$  which must be satisfied for the system to exhibit any growth in  $R$ . It is worth pointing out what happens at the two limiting values of  $r$ , i.e., when it is zero, and one. When  $r \rightarrow 0$ , i.e when one of the decay rates is much smaller than the other, then any small deviation from normality is sufficient for a possibility of transient growth. In the other limit when the decay rates are almost equal,  $r \rightarrow 1$ , the vectors must almost be collinear, the system has to be extremely nonnormal to exhibit any transient growth.

Note that  $r = 0$  implies one of the two vectors stays constant, while  $r = 1$  is a case we have seen in high school to yield transient growth. Indeed the present analysis is not valid at either points. The inequality in Eq (1.6) can be rewritten in terms of cosine as

$$\cos^2\phi < \frac{4r}{(1+r)^2}, \text{ or } \cos\phi = \frac{(1+h)2\sqrt{r}}{1+r}, \quad (1.7)$$

where  $h > 0$ , and  $(h+1) < ((1+r)/(2\sqrt{r}))$ . This strict inequality cannot be satisfied at  $r = 1$ .

Since by definition  $y$  must always be greater than zero for any positive  $C$ . The smaller of the two roots in Eq (1.4) must be greater than zero, so

$$\frac{(1+r)\cos\phi - \sqrt{(1+r)^2\cos^2\phi - 4r}}{2} > 0 \quad (1.8)$$

which means  $r > 0$ .

For a system to have any possible transient growth Eq (1.6) must be satisfied, but transient growth is still not assured that the system will exhibit transient growth. The other parameter which matters is  $C$ , the ratio of the initial vector magnitudes. If the condition for  $\phi$  is satisfied and  $C$  is in the required range, only then are we assured of any growth in  $R$ . In this system,  $C$  is the initial condition. In our toy problem have the liberty to choose the initial conditions to obtain a growth in  $R$ . In contrast real processes always have inherent randomness such that initial conditions are most often random in nature so that they range over a wide spectrum. As a result there is always a possibility of the *right* initial conditions being picked up by the system to exhibit transient growth.

From Eq (1.4) and Eq (1.7) at  $t = 0$  we have

$$C > \frac{1+r}{2\sqrt{r}\sqrt{1+h}(\sqrt{1+h} \pm \sqrt{h})}. \quad (1.9)$$

As  $r$

$\rightarrow 1$   $h \rightarrow 0$  then for any  $C > 1$  we will see transient growth. As  $r \rightarrow 0$  no finite value of  $C$  will give transient growth. This is interesting in view of the fact that when  $r \rightarrow 0$  the condition for  $\phi$  is satisfied very easily but no  $C$  will give transient growth. On the other hand when  $r \rightarrow 1$  the condition on  $\phi$  is not satisfied very easily but is satisfied any  $C > 1$  will give transient growth.

### 1.1.2 Optimal $C$

Once a range of  $C$  over which transient growth is possible is established, the next question to be asked is for what value of  $C$  over this range is the growth maximum. The  $C$  for which the growth is maximum corresponds the optimal initial condition. To arrive at the optimal  $C$  let us define a growth parameter  $G$  as

$$G(t) = \max_{R(0) \neq 0} \left[ \frac{R^2(t)}{R_0^2} \right] \text{ and } G_{max} = \max_t G(t). \quad (1.10)$$

$G$  is now a function of  $t$  and  $C$ , if we set  $dG/dC = 0$  then we arrive at the optimal  $C$  which is a function of  $t$ :

$$C_{opt} = \frac{(1+z) \pm \sqrt{(1+z)^2 + 4z \sin^2 \phi}}{2 \cos \phi} \quad (1.11)$$

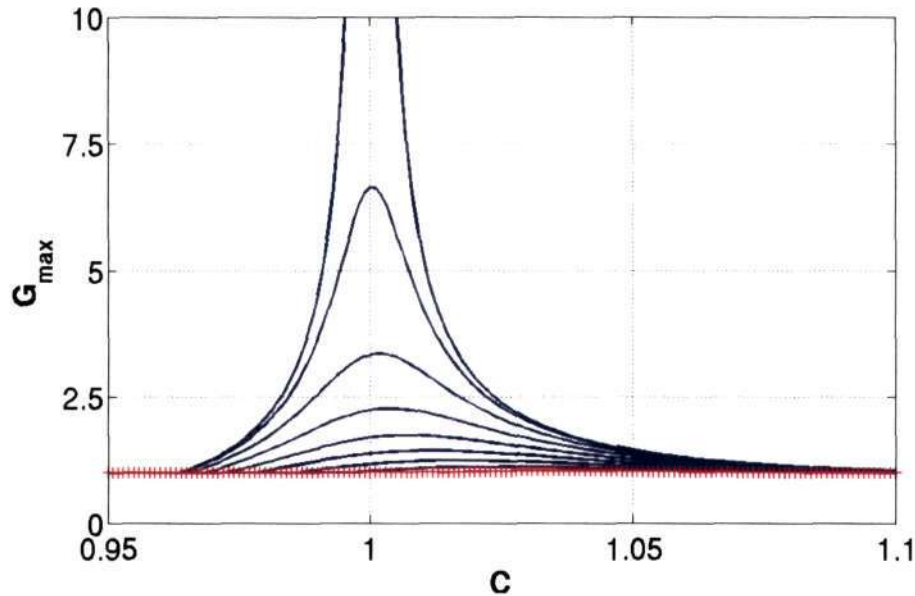


Figure 1.2: The maximum transient growth  $G_{max}$  as a function of the initial ratio  $C$  of the magnitudes of the two vectors. The different lines correspond to various values of the angle  $180 - \phi$  between the vectors, beginning with  $\phi = 0^\circ$  for the topmost curve, and ending with  $\phi = 3.82^\circ$  for the bottom curve shown by the plus symbols. The values of  $\phi$  in between are  $0.42^\circ$ ,  $0.85^\circ$ ,  $1.27^\circ$ ,  $1.69^\circ$ ,  $2.12^\circ$ ,  $2.55^\circ$ ,  $2.97^\circ$  and  $3.39^\circ$  respectively. The bottom curve corresponds to the critical value of  $\phi$ , hence smaller angles between the two vectors would ensure a decay of their resultant.

where  $z$  is evaluated at the given time.  $C_{opt}$  here corresponds to a  $C$  which yields the maximum of all  $G$  at a given time, but it does not give the global maximum of  $G$  over all time. In Eq (1.11)  $C_{opt}$  has two roots, to find which of the two roots is  $C_{opt}$  we check whether  $d^2G/dC^2 < 0$ . It can be shown that greater of the two roots yields a second derivative less than zero, thus  $C_{opt}$  corresponds to greater of the two roots. As an example the variation of  $G_{max}$  with  $C$  is shown in Fig: 1.2 for  $\lambda_1 = 8$  and  $\lambda_2 = 7$ . The figure shows curves for different values of  $\phi$  varying from 0 to the critical value below which transient growth is possible. Note that as  $C$  is increased  $G_{max}$  first increases and then decreases, the value of  $C$  at which  $G_{max}$  attains a maximum is the optimal  $C$ .

We have seen that transient growth is possible in a stable system only under certain conditions; first, that it should be nonnormal and second that it should satisfy the condition on  $\phi$ . Further, the word nonnormality is often used to imply

transient growth in a system but it is now clear from the toy model that this is not always true. Nonnormality is only a necessary condition but not a sufficient condition. A departure from normality will not ensure transient growth unless the condition for  $\phi$  is satisfied which is the sufficient condition. The fact that nonnormality is necessary can be seen if we set  $\phi = 0$  in  $dR/dt$

$$\frac{dR}{dt} = \frac{-1}{R}(C^2\lambda_2e^{-2\lambda_2t} + \lambda_1e^{-2\lambda_1t}) \quad (1.12)$$

which is less than zero for any  $C$  and decay rates.

The condition  $dR/dt > 0$  ensures that  $R$  grows at some point of time in its evolution. A growth in  $R$  at any time  $t > 0$  need not necessarily be greater than  $R_0$ . This is not of great importance. If  $dR/dt|_{t=0} > 0$  then growth in  $R(t > 0)$  will always be more than  $R_0$ . By using this new condition we get a constraint on  $C$

$$C < \frac{1+r}{2r} \left[ \cos \phi \pm \sqrt{\left(\frac{1-r}{1+r}\right)^2 - \sin^2 \phi} \right]. \quad (1.13)$$

The condition for  $\phi$  can also be derived from the above equation as it was from Eq (1.4).

## 1.2 An initial value problem

With the toy model we have illustrated that transient growth is possible in stable systems and under what conditions it is possible. The toy model was considered since we can understand a lot of dynamics from this simple example. In physical systems we come across initial value problems where we are interested in the stability of the system. In this section we intend to show that the toy model was not an abstract example to explain transient growth. The vectors in Fig: 1.1 can be expressed as the eigenvectors of an initial value problem such that the decay rates are the eigenvalues. To see this let us consider an initial value problem of the form

$$\frac{dX}{dt} = \mathcal{A}X, \quad (1.14)$$

where  $X$  is an  $n$  dimensional vector,  $X = [X_1, X_2, \dots, X_n]^T$ . The problem under consideration is autonomous and linear so that  $\mathcal{A}$  is independent of  $t$  and  $X$ . Let us consider a 2 dimensional case so that

$$\mathcal{A} = \lambda_\infty \begin{bmatrix} -1 & p \\ 0 & -r \end{bmatrix}. \quad (1.15)$$

Any 2X2 matrix can be written in the above form by rotating the matrix so that one of its eigenvectors aligns with one of the coordinate axes. Note that this is the canonical form of a nonnormal matrix, a nonnormal matrix would give a triangular matrix upon rotation whereas a normal matrix would lead to a diagonal matrix. In  $\mathcal{A}$  the off-diagonal term would be zero if the matrix were normal, the reason for this will be seen. The eigenvalues of  $\mathcal{A}$  are  $\lambda_1$  and  $\lambda_2$ , if  $\phi$  is defined such that

$$p = \frac{(1-r) \cot \phi}{\lambda_1} \quad (1.16)$$

the eigenvectors of  $\mathcal{A}$  would correspond to the vectors in Fig: 1.1. It is clear now that the toy model represents an initial value problem. If  $\phi = 90^\circ$  then  $p = 0$  resulting in a diagonal matrix, i.e. a normal system. A more formal definition of a normal matrix and a normal operator is discussed by Trefethen and Embree (2005),

- An operator  $L$  is called normal if

$$L^\dagger L(x) = LL^\dagger(x) \quad (1.17)$$

where  $L^\dagger$  is the adjoint of  $L$ , this is a sufficient condition for nonnormality (not for transient growth). Note that  $L = L^\dagger$  is the condition for the operator to be self adjoint, self adjoint operators are also normal, but the converse is not always true.

- Similarly matrix  $M$  is called normal if

$$MM^\dagger = M^\dagger M \quad (1.18)$$

where  $M^\dagger$  is the adjoint of  $M$

We reiterate that nonnormality is necessary but not sufficient for transient growth. A sufficient condition would be similar to that of the toy model,  $dE/dt|_{t=0} > 0$  where  $E$  is energy of the system defined in a way similar to  $R$ . This for operators and matrices translates to

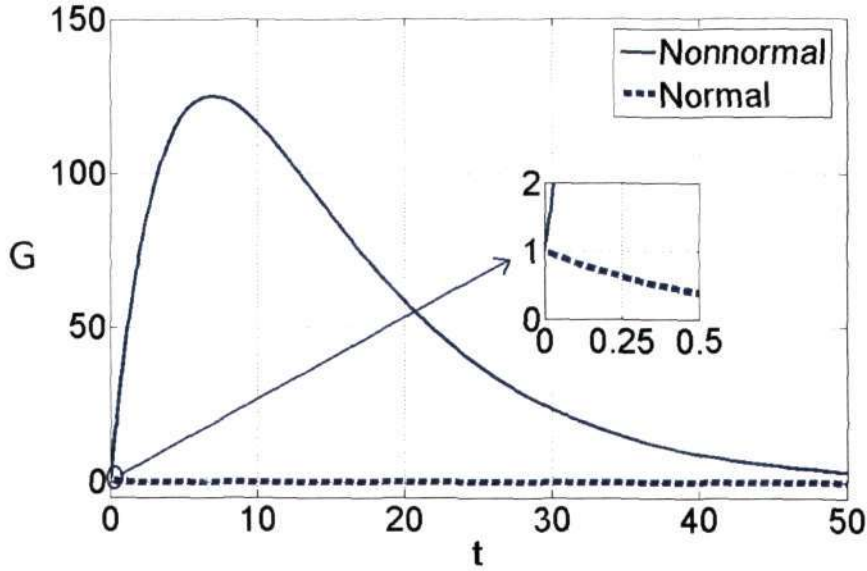


Figure 1.3: Evolution of the optimal growth

$$\lambda_{max}(L + L^\dagger), \lambda_{max}(M + M^\dagger) > 0 \quad (1.19)$$

where  $\lambda_{max}$  implies the largest eigenvalue. This condition if applied to  $\mathcal{A}$  yields the condition for  $\phi$  given in Eq (1.6). The general solution of equation 1.14 is given by

$$x = V_1 e^{\lambda_1 t} + V_2 e^{\lambda_2 t} + \dots \text{ or} \quad (1.20)$$

$$(1.21)$$

for distinct eigenvalues  $\lambda_i$  and  $V_i$  are the corresponding eigenvectors. The case of repeated eigenvalues is not discussed here, but similar dynamics are displayed there too.

We are interested in a case where all the eigenvalues are negative, we take two example matrices for  $\mathcal{A}$ , with negative eigenvalues. In our example, we set  $N = 2$  for simplicity, but our conclusions hold good for large  $N$  as well.



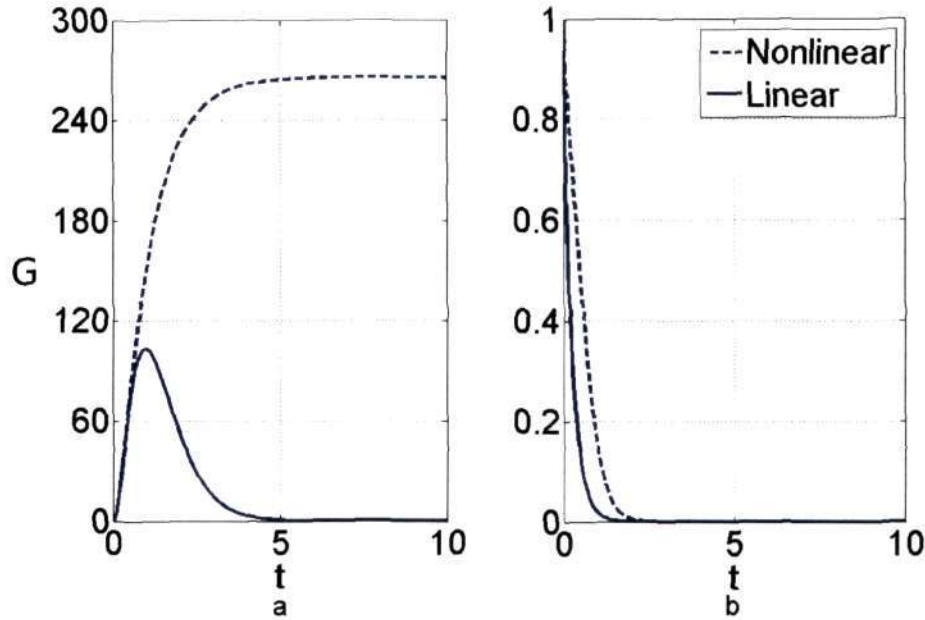


Figure 1.4: Linear and nonlinear evolution of normal and nonnormal matrices

$$\mathcal{A}_\infty = \begin{bmatrix} -8 & 100 \\ 0 & -7 \end{bmatrix} \text{ and } \mathcal{A}_\epsilon = \begin{bmatrix} -10 & 5 \\ 5 & -5 \end{bmatrix} \quad (1.22)$$

In the example,  $\mathcal{A}_\infty$  is nonnormal and  $\mathcal{A}_\epsilon$  is normal.  $\mathcal{A}_\infty$  in addition Eq (1.19) which is a sufficient condition for transient growth. Let us define the energy of the system,  $E$ , as the sum of squares of components of the vectors  $X$  and  $G$  as defined in Eq (1.10) is the ratio of energy at any time to the initial energy. In Fig: 1.3(a) and (b) respectively the evolution of  $G$  for  $\mathcal{A}_\infty$  and  $\mathcal{A}_\epsilon$  are shown.

In stability analysis most often the nonlinear terms are neglected and a linear stability analysis is carried out. If however the system displays a large transient growth, we can see different dynamics upon including the nonlinear terms. Consider a nonlinear equation

$$\frac{dX}{dt} = AX - BX^2 \quad (1.23)$$

The system has two stable states one at  $X = 0$  and the other at  $AX = BX^2$ . At small time when  $X$  is small the nonlinear term is not important but when  $X$  is large it can take the system to a new state. In Fig: 1.4 we can see that the

nonlinear term, aided by the transient growth at short times, has led the system to a new state. Matrix  $B$  is taken to be

$$B = \begin{bmatrix} 0.005121 & 5 \\ 0 & 0 \end{bmatrix} \quad (1.24)$$

With this as a background, we move on to examine simple shear flows.

## CHAPTER 2

# ALGEBRAIC INSTABILITY IN INVISCID STRATIFIED SHEAR FLOWS

Analysis of an inviscid flow can reveal a lot about the dynamics of a problem . In this chapter we study analytically a simple inviscid stratified shear flow. We try to explore this problem to probe into the short time dynamics of perturbations to the flow.

### 2.1 Introduction

One of the interesting features of atmospheric and oceanic flows are that they are commonly characterized by stable stratification. Very rarely does an unstable stratification occur in oceans. The upper atmosphere, stratosphere and planetary boundary layers have stable stratification, see fig: 2.1. Thus stratified flows are very common in geophysical flow. Gravity effects play an important role on these flows.

Atmospheric flows are generally modeled as being bounded on one side and unbounded on the other. In this work we consider a flow bounded on both sides. We deal with stratified Couette flow, fig: 2.2 shows the schematic. It turns out that the mechanism of algebraic instability is more or less be the same in both bounded and unbounded flows. The work done in this Chapter is in collaboration with Anubhab Roy.

We begin with the derivation of the linear stability equations in the inviscid framework. The stability of a flow can be studied by introducing small perturbations to the flow and studying how they evolve. The governing equations are the continuity equation, the Navier-Stokes equation and the heat equation which in this case is the temperature advection diffusion equation. The Boussinesq approximation is made, i.e. density variations are considered important only in the buoyancy term of the Navier-Stokes equation. Flow quantities can be split into mean+perturbation as  $\tilde{U} = U + \tilde{u}$ ,  $\tilde{P} = P + \tilde{p}$ ,  $Te = \bar{T} + \tilde{T}$ . Writing the governing equations for total flow quantities and subtracting the equations for mean

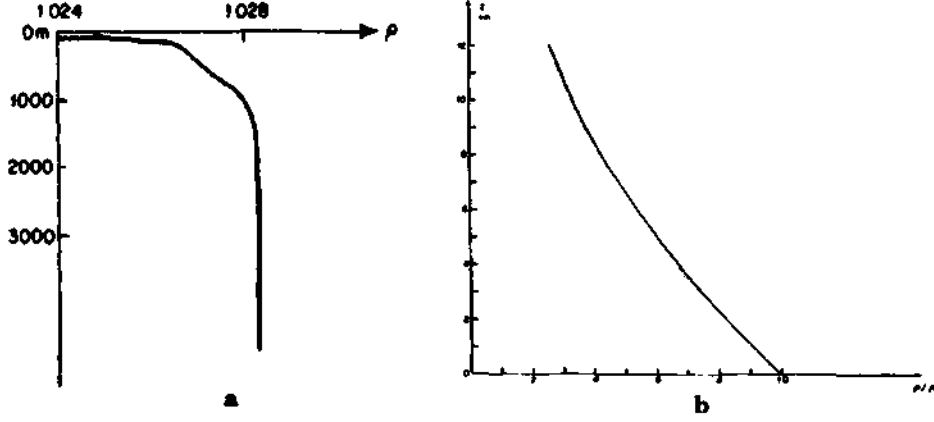


Figure 2.1: Stratification profiles a) with depth in oceans b) with height in the atmosphere (Pedlosky (1986))

from these we get equations for the perturbation. If the perturbations are small enough then nonlinear terms may be neglected which gives the linearized perturbation equations. Let the mean flow be only in  $x$  direction and vary only along  $y$  such that  $\bar{U} = U(y)i$ . The stratification is taken to be linear such that mean temperature varies linearly along  $y$ ,  $\bar{T} = ay$ . Substituting these into the linearized perturbation equation of velocity and temperature, we get in non-dimensional form,

$$\frac{\partial \tilde{u}}{\partial t} + U \frac{\partial \tilde{u}}{\partial x} + \tilde{v} U' = -\frac{\partial \tilde{p}}{\partial x} + \frac{1}{Re} \nabla^2 \tilde{u} \quad (2.1)$$

$$\frac{\partial \tilde{v}}{\partial t} + U \frac{\partial \tilde{v}}{\partial x} = -\frac{\partial \tilde{p}}{\partial y} + \frac{1}{Re} \nabla^2 \tilde{v} - Ri \tilde{T} \quad (2.2)$$

$$\frac{\partial \tilde{w}}{\partial t} + U \frac{\partial \tilde{w}}{\partial x} = -\frac{\partial \tilde{p}}{\partial z} + \frac{1}{Re} \nabla^2 \tilde{w} \quad (2.3)$$

$$\frac{\partial \tilde{T}}{\partial t} + U \frac{\partial \tilde{T}}{\partial x} + \tilde{v} \bar{T}' = \frac{1}{Re Pr} \nabla^2 \tilde{u}. \quad (2.4)$$

Velocity and pressure perturbation are represented in lowercase with superscript tilde and mean velocity in uppercase.  $T$  is the perturbation temperature and  $\bar{T}$  is the mean temperature. The prime denotes differentiation with respect to  $y$ . Taking divergence of the momentum equations and using the continuity equation we get an equation for pressure

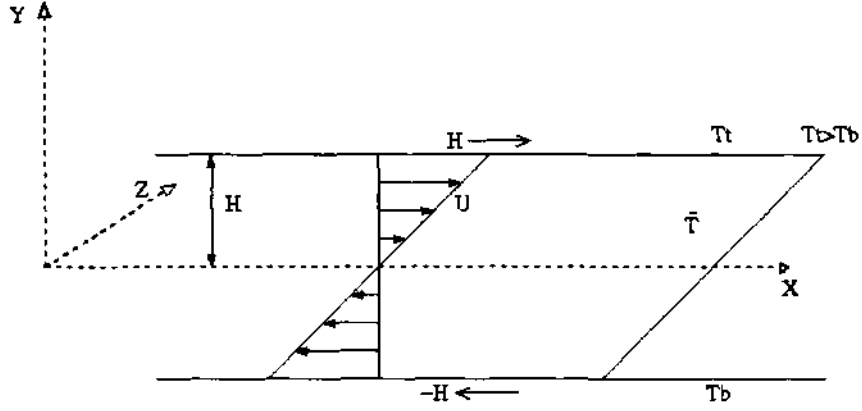


Figure 2.2: Schematic of stably stratified Couette flow

$$\nabla^2 \tilde{p} = -2U' \frac{\partial \tilde{v}}{\partial x} + Ri \frac{\partial \tilde{T}}{\partial y} \quad (2.5)$$

Take the divergence of  $\tilde{v}$  momentum equation and using the above equation to eliminate  $\tilde{p}$  we get an equation for wall normal velocity

$$\left[ \left( \frac{\partial}{\partial t} + U \frac{\partial}{\partial x} \right) \nabla^2 - U'' \frac{\partial}{\partial x} - \frac{1}{Re} \nabla^4 \right] \tilde{v} = Ri \left( \frac{\partial^2}{\partial x^2} + \frac{\partial^2}{\partial z^2} \right) \tilde{T}. \quad (2.6)$$

A second equation is needed to describe the other two velocities. The wall normal vorticity is defined as

$$\tilde{\eta} = \frac{\partial \tilde{u}}{\partial z} - \frac{\partial \tilde{w}}{\partial x}, \quad (2.7)$$

an equation in terms of  $\tilde{\eta}$  will contain information about both  $\tilde{u}$  and  $\tilde{w}$ . By differentiating Eq (2.1) with respect to  $z$ , differentiating Eq (2.3) with respect to  $x$  and subtracting the latter from the former we get an equation for the wall normal vorticity

$$\left[ \left( \frac{\partial}{\partial t} + U \frac{\partial}{\partial x} \right) - \frac{1}{Re} \nabla^2 \right] \tilde{\eta} = -U' \frac{\partial \tilde{v}}{\partial z} \quad (2.8)$$

The flow is periodic in  $x$  and  $z$  direction hence a Fourier transformation may be used in these directions. The Fourier transformation is of the form

$$[\tilde{u}, \tilde{\eta}, \tilde{T}](x, y, z, t) = \int_{-\infty}^{\infty} \int_{-\infty}^{\infty} [u, \eta, T](y, t) e^{i(\alpha x + \beta z)} d\alpha d\beta \quad (2.9)$$

We can thus write the stability equations in normal mode form, with a wave

number  $\alpha$  in  $x$  direction and  $\beta$  in the  $z$  direction, for velocity, vorticity and temperature as

$$\left[ \left( \frac{\partial}{\partial t} + i\alpha U \right) (D^2 - k^2) - i\alpha U'' - \frac{1}{Re} (D^2 - k^2)^2 \right] v = k^2 Ri T \quad (2.10)$$

$$\left[ \left( \frac{\partial}{\partial t} + i\alpha U \right) - \frac{1}{Re} (D^2 - k^2) \right] \eta = -i\beta U' v \quad (2.11)$$

$$\left[ \left( \frac{\partial}{\partial t} + i\alpha U \right) - \frac{1}{Re Pr} (D^2 - k^2) \right] T = -\bar{T}' v, \quad (2.12)$$

where  $k^2 = \alpha^2 + \beta^2$  and  $D = \frac{\partial}{\partial x}$ . The above equations completely describe the evolution of perturbation in a stratified parallel flow. As our interest in this chapter lies in the 2D inviscid framework we drop the diffusion terms and the vorticity equation to arrive at the inviscid Rayleigh equation and the temperature advection equation. We deal with stratified Couette flow with a simple shear of form  $U = y$  and as mentioned earlier the temperature profile has the form  $\bar{T} = y$ . The perturbation temperature is thus nondimensionalized by  $\Delta T$ , the temperature difference between the two walls.

$$\left[ \left( \frac{\partial}{\partial t} + i\alpha U \right) (D^2 - \alpha^2) \right] v = \alpha^2 Ri T \quad (2.13)$$

$$\left[ \left( \frac{\partial}{\partial t} + i\alpha U \right) \right] T = -\bar{T}' v \quad (2.14)$$

The non dimensional numbers used in the equations are defined as

- Reynolds number:  $Re = \frac{\text{Inertia force}}{\text{viscous force}} = \frac{U_c H}{\nu}$
- Prandtl number:  $Pr = \frac{\text{Viscous Diffusion rate}}{\text{Thermal Diffusion rate}} = \frac{\nu}{k_T}$
- Grashof number:  $Gr = \frac{\text{Buoyancy force}}{\text{Viscous force}} = \frac{g\alpha_T \Delta T H^3}{\nu^2}$
- Richardson number:  $Ri = \frac{\text{Potential Energy}}{\text{Kinetic Energy}} = \frac{Gr}{Re^2} = \frac{g\alpha_T \Delta T H}{U_c^2}$

where  $U$  is the characteristic velocity,  $H$  is a characteristic width in the flow,  $k_T$  is the thermal diffusivity,  $\alpha_T$  is the coefficient of thermal expansion and  $g$  is acceleration due to gravity. In Couette flow, which we are considering,  $U_c$  is velocity at the walls and  $H$  is half channel height.

## 2.2 Stability of Stratified Shear Flow

Stability of atmospheric flow is a problem of great interest in geophysical flows. Stability of stratified atmospheric flow, modeled as both bounded and unbounded flow, is a well studied problem in literature. The earliest work on this was done by Taylor (1931) and Goldstein (1931) who independently modeled the stratified atmospheric flow and arrived at the now well known Taylor-Goldstien equation the name for which was coined by Drazin. An in-depth analysis of the problem was first done by Eliassen, Hoiland & Riis (1953). They studied the problem for all possible range of Richardson number ( $Ri$ ), stable and unstable. Apart from obtaining the eigen solutions of the problem the main interest was in arriving at the asymptotic time exponents, which they obtain for a range of  $Ri$ . At  $Ri = 0$ , i.e. unstratified case, the exponent matches with the that of Case (1960a).

There had been a debate about the correct exponent of  $t$  until Brown & Stewartson (1980) derived the correct exponent. Case (1960b) arrived at an exponent which was shown to be incorrect. Booker & Bretherton (1967) who study the problem of internal gravity waves also arrive at an exponent of  $t$  which confirmed by Brown and Stewartson (1980). Banks, Drazin & Zaturka(1976) analyze the normal modes of flow, they divide the normal modes in 5 categories for a given wave number and study them, but do not attempt to arrive at any large time exponents. A later result by Chimonas (1979) for the time exponent, which was conflicting with Case's (1960b) work, was shown to be in correct by Brown & Stewartson (1980).

It was not until the early 1990's that the transient stability of the problem was addressed. Farrel & Ioannou (1993) numerically studied the transient algebraic growth in the 2D inviscid problem for both bounded and unbounded couette flow by giving optimal excitation to the flow. The full 3D viscous problem was studied by Bakas, Ioannou & Kefaliakos (2001) who again use the optimal excitation technique to study the transient growth for the unbounded case and show that streamwise

| Author                             | Flow Regime            | Transient or $t \gg 1$       |
|------------------------------------|------------------------|------------------------------|
| Eliassen, Hoiland & Riis (1953)    | Unbounded              | $t \gg 1$                    |
| Dikii (1960)<br>Case/Dyson, (1960) | Unbounded              | $t \gg 1$                    |
| Kuo, 1963                          | Bounded & Unbounded    | $t \gg 1$                    |
| Booker & Bretherton (1967)         | Unbounded              | $t \gg 1$                    |
| Chimonas, 1979                     | Unbounded              | $t \gg 1$                    |
| Brown & Stewartson, 1980           | Unbounded              | $t \gg 1$                    |
| Farrel & Ioannou, 1993             | Bounded & Unbounded    | <b>Transient (numerical)</b> |
| Bakas, Ioannou & Kefaliakos, 2001  | Unbounded, 3D, Viscous | <b>Transient (numerical)</b> |

Figure 2.3: A brief literature survey

rolls are the ones that grow optimally. The table in Fig. 2.3 show a brief list of work done on this problem. The red colour in the third column indicates inconstancy in the exponent obtained by the authors, dark blue indicates the correct results and black indicates that the work is numerical. The light blue in column two is for 2D inviscid cases and brown for 3D viscous case.

## 2.3 An Analogy

Transient algebraic instability was analytically shown for the first time by Landahl (1980) based on Case's (1960) work on inviscid Couette flow. The main focus of Case's (1960) work was to show that while no discrete solution exist in a plane Couette flow, a continuous spectrum exists. This is an important result of Case with far reaching consequences for an algebraic growth. It was later shown by Landahl (1980) that an algebraic growth is possible in the wall normal vorticity. If the flow is in zero gravity we can treat temperature field as a passive scalar and the  $T$  term can be dropped in  $Q$  (2.10), then 2D stratified passive scalar Couette



flow and the unstratified 3D Couette flow have very similar governing equations.

The governing equations for the perturbation velocity for both the cases are the identical. The wall normal vorticity equation for unheated Couette flow and the temperature perturbation equation for 2D stratified passive scalar Couette flow have a striking similarity.

$$\left[ \left( \frac{\partial}{\partial t} + i\alpha U \right) \right] \eta = -i\beta U' v \quad (2.15)$$

$$\left[ \left( \frac{\partial}{\partial t} + i\alpha U \right) \right] T = -\bar{T}' v \quad (2.16)$$

The only difference between the above equations is the factor  $i\beta$ , as both  $U$  and  $T$  have the same profile. If we set  $\beta = 1$  equations in  $i\eta$  and  $T$  are identical.

Landahl's proof for algebraic instability in wall normal vorticity can be extended to the stratified case without gravity (passive scalar). Since we are discussing an initial value problem we take a Laplace transform in time instead of the usual Fourier transform to get

$$(D^2 - k^2)\hat{v} = \frac{\hat{\phi}_0}{S + i\alpha U} \quad (2.17)$$

where hat quantities represent Laplace transformed variables,  $S$  is the Laplace transform variable and  $\hat{\phi}_0 = (D^2 - k^2)v(0)$ . Introducing the Green's function  $G(y|y')$

$$\hat{v} = \int_{-1}^1 G(y|y') \hat{\phi}_0 dy'. \quad (2.18)$$

Using boundary condition for the greens function as  $G(y, y') = 0$  at  $y = 0, 1$  we get

$$G(y|y') = \begin{cases} \frac{-\sinh k(1-y) \sinh k(1+y')}{k \sinh k} & y' < y \\ \frac{-\sinh k(1+y) \sinh k(1-y')}{k \sinh k} & y' > y \end{cases} \quad (2.19)$$

The solution of Eq (2.17), after inverting the Laplace transform, can be written as

$$v = \int_{-1}^1 G(y|y') \phi_0 e^{-i\alpha t y'} dy' \quad (2.20)$$

which is clearly a decaying solution. But as mentioned earlier the growth occurs in wall normal vorticity. Taking the Laplace transform of Eq (2.15) we get

$$\hat{\eta} = \frac{\eta_0}{S + i\alpha y} - \frac{-i\beta U'v}{S + i\alpha y}. \quad (2.21)$$

where  $\eta_0$  is the initial vorticity. Inverting the Laplace transform we get

$$\eta = \eta_0 e^{-i\alpha y t} - i\beta U' \int_0^t v(y, t') e^{-i\alpha y t'} dt'. \quad (2.22)$$

substituting the solution for  $v$  from Eq (2.20) into the above equation and Taylor expanding the exponential for small time, the above equation can be written as (see Schmid & Henningson, 2001)

$$\eta \simeq \eta_0 e^{-i\alpha y t} - i\beta U' v_0 t - i\beta U' \alpha t^2 \left[ y v_0 + \int_{-1}^1 \frac{\partial G}{\partial y'} v_0 dy' \right] \quad (2.23)$$

It can clearly be seen that there is an algebraic growth in wall normal vorticity at small times. Note that the above equation is valid only for small times and that this growth is purely because of the flow being 3D. The solution will be drastically different if  $\alpha = 0$ , solution for  $\eta$  has to arrived at from Eq (2.22). There will be an algebraic instability in  $\eta$ . At large time an unbounded linear growth in time can be seen, as shown by Elingson & Palm(1975). In the stratified case the solution for  $T$  will be not any different from that of  $\eta$  for non-zero  $\alpha$ . Based on the analogy between  $\eta$  and  $T$  replace  $i\beta U'$  by  $\bar{T}'$  to get the solution for  $T$

$$T \simeq T_0 e^{-i\alpha y t} - \bar{T}' v_0 t - \bar{T}' \alpha t^2 \left[ y v_0 + \int_{-1}^1 \frac{\partial G}{\partial y'} v_0 dy' \right] \quad (2.24)$$

where  $T_0$  is the initial temperature perturbation. In stratification case the temperature grows similar to  $\eta$  but the flow is only 2D. In unheated flow transient growth is mainly a 3D phenomenon, wall normal vorticity is required for lift up mechanism to occur which is the physical mechanism of transient growth. The lift up mechanism will be explained in the next chapter. But with stratification, interestingly, lift up mechanism is no longer necessary for transient growth, there seems to be a different mechanism causing growth in the 2D stratified flow which needs to be explored. Note that all of the arguments made are for a passive scalar but when gravity is considered in the equation for wall normal velocity we believe that a growth in  $v$  should be possible, this is the topic of discussion in the following

section.

## 2.4 Transient Growth Mechanism

Most often when dealing with nonnormality and transient growth in a system the natural questions that are raised are, what is the optimal growth, How nonnormal is the system, etc. In dealing with these questions one should not forget the underlying physical mechanisms of transient growth. The physical mechanisms of transient growth in wall bounded flows have been well studied. Although the concept of transient growth had not yet originated by then, Orr had discussed the mechanism of growth of spanwise vorticity as early as 1907 (Orr 1907). The lift-up effect, a 3D mechanism of transient growth was explained by Landahl (1980). We shall first discuss the lift up mechanism of transient growth and then discuss the Orr mechanism for 2D transient growth in inviscid flows.

The process of generation of horizontal perturbation velocity from the mean flow by displacing (lifting up and pushing down) of fluid particles is termed as the lift-up effect. The lift-up effect requires perturbation velocities in the spanwise direction, hence it is a 3D mechanism of transient growth. To understand the lift-up effect consider Fig. 2.4, where the over bar represent mean quantities and terms with tilde are perturbations. The sinusoidal waves in the figure are Fourier perturbation waves in the spanwise direction and the mean flow is shown to have simple shear velocity profile(Couette Flow), but one can consider a parabolic velocity for the mean flow and the explanation will remain the same. The base state vorticity  $U'$  in the spanwise direction can be stretched or compressed by variation of  $\tilde{u}_z$  in the z direction to generate the perturbation vorticity in spanwise direction. The Fourier perturbation waves are introduced both in stream wise and spanwise direction. The gradient of streamwise perturbation velocity in the z-direction stretches and tilts the base state vorticity about the y-axis to generate a perturbation vorticity,  $\tilde{\omega}_x$ , in the streamwise direction. Similarly the gradient of the perturbation wall normal velocity in the z direction stretches and tilts the base state vorticity about x-axis to generate wall normal perturbation vorticity,  $\tilde{\omega}_y$ . The perturbation vorticity in the wall normal direction is in turn stretched and tilted by the gradient of  $\bar{U}$  (mean velocity in x direction) about the z axis which generates perturbation vorticity in streamwise direction. Perturbation velocities in wall normal and spanwise

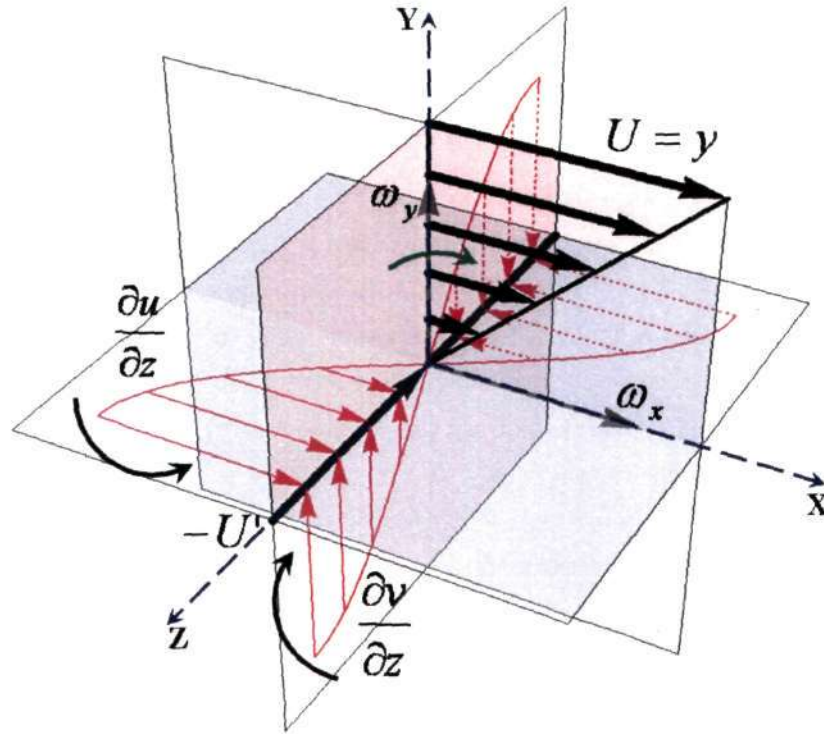


Figure 2.4: Illustration of the Lift-up effect. Figure courtesy Anubhab Roy

direction result from the perturbation vorticity in streamwise direction, velocities in spanwise and streamwise direction result from wall normal perturbation vorticity. Thus, with the initial disturbance interacting with the mean, more perturbation is generated from the mean which is a cyclic process because the newly generated perturbation interact with mean to generate even more perturbation. Another explanation which continues from the above explanation (see, e.g. Trefethen et. al. (1993)) is that streamwise rolls (streamwise perturbation vorticity) lift up and push down fluid packets to create elongated regions of low and high velocity (perturbation velocity in stream wise direction) in the mean flow resulting in the streamwise streaks which are well observed features in laboratory experiments involving wall bounded an boundary layer flows.

The lift-up mechanism explains why we observe transient growth in a 3D flow, but it does not explain the mechanism of transient growth in a 2D flow. The 2D

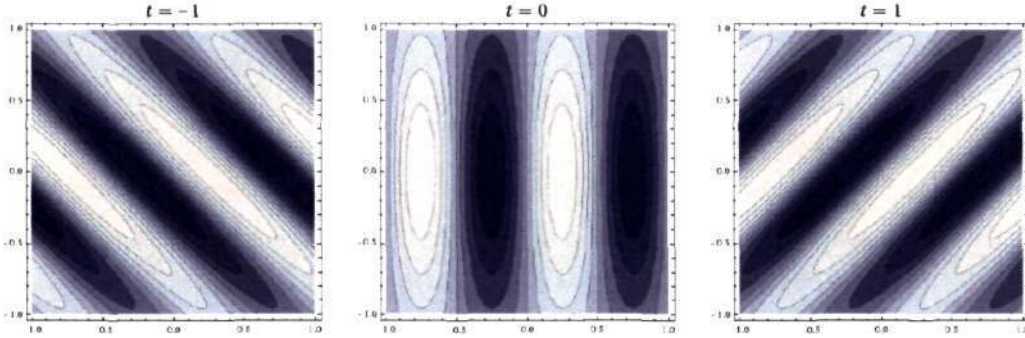


Figure 2.5: Orr-Mechanism of transient growth in a 2D flow.

transient growth can be understood through the Orr mechanism (Farrel & Ioannou, 1993) or the Reynolds stress mechanism which are very intuitive. Consider the equation for the evolution of perturbation energy

$$\frac{\partial E}{\partial t} = -\frac{1}{2} \int U' \langle uv \rangle dy = \frac{1}{2} \int \bar{U}' \left\langle \frac{\partial \psi}{\partial y} \frac{\partial \psi}{\partial x} \right\rangle dy = -\frac{1}{2} \int \left( \frac{\partial y}{\partial x} \right)_\psi \left( \frac{\partial \psi}{\partial y} \right)^2 dy. \quad (2.25)$$

Consider again a simple shear flow. Fig. 2.5 shows perturbation of spanwise vorticity at different instants of time. At time  $t = -1$  the vortex patch is tilted to the left, the mean shear tilts the vortex patch to the right and becomes more compact during which the vortex patch gains energy from the mean and reaches a peak at  $t = 0$ . For  $t > 0$  the patch is tilted and stretched to the right by the mean shear during which it starts losing energy to the mean flow. Thus for  $-1 < t < 0$  there is a transient growth in energy of the perturbation and for  $t > 0$  the energy decays. We can also see this from Eq (2.25), when the vortex is tilted to right from its left inclination (negative tilt) then  $(\partial y / \partial x)_\psi \bar{U}' < 0$  or  $\langle uv \rangle < 0$  which means  $\partial E / \partial t > 0$  hence energy grows. When the vortex patch is tilted to the right from zero tilt inclination, i.e. once it has a positive tilt, then  $(\partial y / \partial x)_\psi \bar{U}' > 0$  thus  $\partial E / \partial t < 0$  as result energy decays for all  $t > 0$ . A mechanism for the temperature driven growth is being worked on.

## 2.5 Algebraic Growth

In the previous section it was shown that an algebraic growth is possible in the perturbation temperature, which was a passive scalar. However in the absence of gravity any changes in the temperature will not affect the flow. Thus we must consider gravity effects to study the effect of temperature on the velocity field. Substantial amount of work has been done on this problem for both bounded and unbounded flows, but the interest lay in the asymptotic growth rates. We look here at small time algebraic growth.

Henceforth in this chapter the stability equations shall be considered in terms of stream function instead of wall normal velocity. For 2D inviscid stratified Couette flow the stability equations will be

$$\left(\frac{\partial}{\partial t} + U \frac{\partial}{\partial x}\right) \nabla^2 \tilde{\psi} = - Ri \frac{\partial \tilde{T}}{\partial x} \quad (2.26)$$

$$\left(\frac{\partial}{\partial t} + U \frac{\partial}{\partial x}\right) \tilde{T} + \tilde{T}' \frac{\partial \tilde{\psi}}{\partial x} = 0. \quad (2.27)$$

We have assumed a linear shear flow and a linear temperature profile, thus with  $U = y$  and  $\tilde{T}' = 1$  the above equations can be reduced into a single equation for  $\psi$

$$\left(\frac{\partial}{\partial t} + y \frac{\partial}{\partial x}\right) \nabla^2 \tilde{\psi} = Ri \frac{\partial^2 \tilde{\psi}}{\partial x^2}. \quad (2.28)$$

Upon Fourier transforming in the streamwise direction and Laplace transforming in time we get

$$\left[ \frac{d^2}{dy^2} - k^2 - \frac{k^2 Ri}{(S +iky)^2} \right] \hat{\psi} = - \frac{\omega_z(0)}{(S +iky)} + \frac{ik Ri}{(S +iky)^2} T(0) \quad (2.29)$$

where the hat represents a Laplace transformed quantity and tilde represents a Fourier transform.  $\tilde{\omega}_z(0)$  is the initial span wise vorticity,  $\tilde{T}(0)$  is initial temperature perturbation and note that  $\beta = 0$  hence  $k = \alpha$ . The homogeneous part of the above equation is called Taylor-Goldstein (Banks, Drazin & Zaturka 1976) equation. The homogenous solutions of the above equation are

$$\hat{\psi}_1 = \sqrt{\xi} I_n(\xi) \quad (2.30)$$

$$\hat{\psi}_2 = \sqrt{\xi} K_n(\xi). \quad (2.31)$$

where  $\xi = -i(S +iky)$ ,  $n = \sqrt{\frac{1}{4} - Ri}$  and  $I_n$  and  $K_n$  are Bessel functions of the first and second kind respectively. Clearly the solution of Eq (2.29) is far more complex than Case's (1960) solution where the greens function contains sine and cosine hyperbolic functions. To motivate the work let us first consider the toy problem given by Brown and Stewartson (1979) for unbounded flow with the difference that we prescribe a bounded flow.

### 2.5.1 Toy Problem: Brown and Stewartson(1979)

Consider Eq (2.29). Dropping the third term on the LHS would be equivalent to considering the Rayleigh equation forced by temperature perturbation, with a uniform base temperature.

$$\left[ \frac{d^2}{dy^2} - k^2 \right] \hat{\psi} = -\frac{\bar{\omega}_z(0)}{(S +iky)} + \frac{ikRi}{(S +iky)^2} \tilde{T}(0) \quad (2.32)$$

The advantage of dropping the mean stratification term is that the Green's function is the same as in unheated Couette flow. The toy problem is similar to unheated Couette flow except here we have a initial temperature perturbation in the flow. For a domain from -1 to 1 the Green's function is given by Eq (2.19). The solution for the stream function is given by

$$\psi = \frac{1}{2\pi i} \int_{c-i\infty}^{c+i\infty} \int_{-1}^1 G(y|y') \left\{ -\frac{\omega_z(0)}{(S +iky')} + \frac{ikRi}{(S +iky')^2} T(0) \right\} e^{St} dy' dS \quad (2.33)$$

After evaluating the contour integral in  $dS$ , integrating the remainder in  $dy'$  by parts we may write at large times,

$$\begin{aligned}
\psi k \sinh k &= \left[ \frac{e^{-iky't}}{ikt} f \sinh k(1+y') \sinh k(1-y) \right]_{y'=-1}^{y'=y} \\
&- \left[ \frac{e^{-iky't}}{k^2 t^2} \frac{d}{dy'} (f \sinh k(1+y') \sinh k(1-y)) \right]_{y'=-1}^{y'=y} + O\left(\frac{1}{t^3}\right) \\
&+ \left[ \frac{e^{-iky't}}{ikt} f \sinh k(1+y') \sinh k(1-y) \right]_{y'=y}^{y'=1} \\
&- \left[ \frac{e^{-iky't}}{k^2 t^2} \frac{d}{dy'} (f \sinh k(1+y') \sinh k(1-y)) \right]_{y'=y}^{y'=1} + O\left(\frac{1}{t^3}\right) \quad (2.34)
\end{aligned}$$

where  $f = -\tilde{\omega}_z(0) + ikRi\tilde{T}(0)t$ . In the above equation the  $O(1/t)$  terms cancel each other leaving only the  $O(1/t^2)$  terms. For large  $t$  and for a general smooth initial condition the stream function can be approximated as

$$\begin{aligned}
\psi &\sim \frac{1}{k^2 t^2} e^{-iky't} f \\
\psi &\sim e^{-iky't} \left\{ \Omega_z O\left(\frac{1}{t^2}\right) + \theta O\left(\frac{1}{t}\right) \right\} \quad (2.35)
\end{aligned}$$

where  $O(1/t^2)$  decay rate corresponds to smooth initial vorticity perturbation ( $\Omega_z$ ) and  $O(1/t)$  decay corresponds to smooth initial temperature perturbation ( $\theta$ ). We next consider initial vorticity perturbation and initial temperature perturbation in the form of delta functions. Let

$$\omega_z(0) = \Omega_z \delta(y' - y_1) \text{ and } T(0) = \theta \delta(y' - y_1). \quad (2.36)$$

Using the above initial conditions, after inverting Laplace transform, in Eq (2.33) we get the solution for  $\psi$  as

$$\psi = G(y|y_1) e^{-iky_1 t} \{-\Omega_z + \theta ikRit\} \quad (2.37)$$

If there is no initial temperature perturbation then  $\tilde{\psi} = -G(y|y_1) e^{-iky_1 t} \Omega_z$  from which it can be seen that stream function has a continuous spectrum oscillating mode. But if we have initial temperature perturbation then the solution is given by



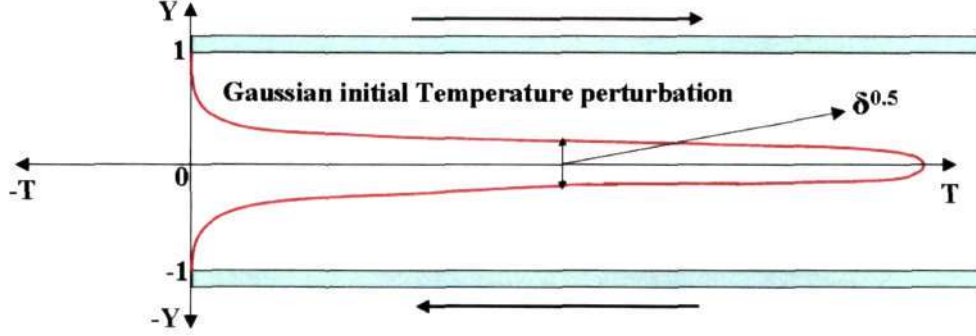


Figure 2.6: Temperature perturbations Profiles

$$\tilde{\psi} \sim te^{-iky_1 t}, \quad (2.38)$$

the stream function shows an unbounded linear growth. Thus a temperature sheet leads to a linear growth of the velocity field. Instead of a delta function if a very thin Gaussian temperature perturbation, of small lateral extent, is introduced, then the stream function would experience growth up to a time which is inversely proportional to the thickness of the Gaussian before the  $O(1/t)$  decay. In Fig. 2.6 both delta and Gaussian temperature perturbations are shown. To show the transient algebraic growth in  $\psi$  and the energy consider a Gaussian for the initial temperature perturbation

$$\tilde{T}(0) = \frac{1}{\sqrt{2\pi\delta}} e^{-\left(\frac{y-y_1}{2\sqrt{\delta}}\right)^2} \quad (2.39)$$

where  $\sqrt{\delta}$  is the lateral extension of the Gaussian, with its peak at  $y_1$ . Fig. 2.7 the response of the stream function at time  $t=5$ , for a Gaussian initial condition in temperature peaked at  $y = 0.25$ , the maximum value of  $\psi$  is 0.4. Fig. 2.8 shows the stream function at  $t=22$  where the increase in stream function can be clearly seen, the maximum value of  $\psi$  is now 1. The evolution of kinetic energy for a pure vorticity perturbation is shown in Fig. 2.9 and for a pure thermal perturbation is shown in fig. 2.10, where  $\delta = 1/1000$ . Algebraic growth occurs only for the thermal perturbation.

To understand how the growth occurs consider a wave packet of perturbation

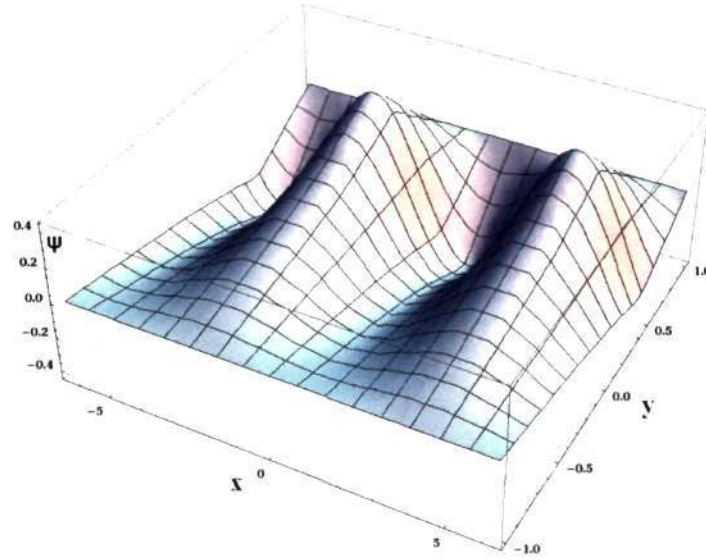


Figure 2.7: Stream function at  $t=5$  for a pure thermal perturbation.

temperature in the small region of thickness  $\sqrt{\delta}$  where temperature perturbation is introduced. In Fig. 2.11 we can see three waves in the packet, one at  $y = 0$ , another at  $y = \sqrt{\delta}/2$  and the third at  $y = -\sqrt{\delta}/2$ . As the streamwise velocity is linear in  $y$  the top wave will move with  $U = \sqrt{\delta}/2$ , the middle wave will remain stationary and the bottom wave will move with  $U = -\sqrt{\delta}/2$ . At  $t = 0$  the waves are in phase thus interference would lead to increase in stream function, with time as they start going out of phase the waves start interacting destructively. At  $t = 1/(\sqrt{\delta}/2)$  the waves will be completely out of phase as shown in the same figure. Thus growth, which is possible only during initial short period of time before the destructive interference sets in, occurs up to  $t = 2/\sqrt{\delta}$  beyond which destructive interference leads to  $O(1/t)$  decay. In Fig. 2.12 variation of time at which maximum growth occurs with  $1/\sqrt{\delta}$  is shown, the exponent of the power law fit on the curve is 0.516. Thus as argued in the wave packet example the time upto which growth occurs is proportional to the inverse of the width of the Gaussian.

The energy in the toy problem is the kinetic energy of the perturbation. From the dependence of  $t_{max}$  on the width of the Gaussian we can predict how the maximum energy would vary with the width of the Gaussian. As  $t_{max}$  is proportional to the inverse of the width so would the velocity be. The maximum energy thus would be proportional to the square of inverse of the width,  $E_{max} \propto 1/\delta$ . From the plot of  $E_{max}$  vs  $1/\delta$ , in Fig. 2.13, the above argument is reconfirmed.

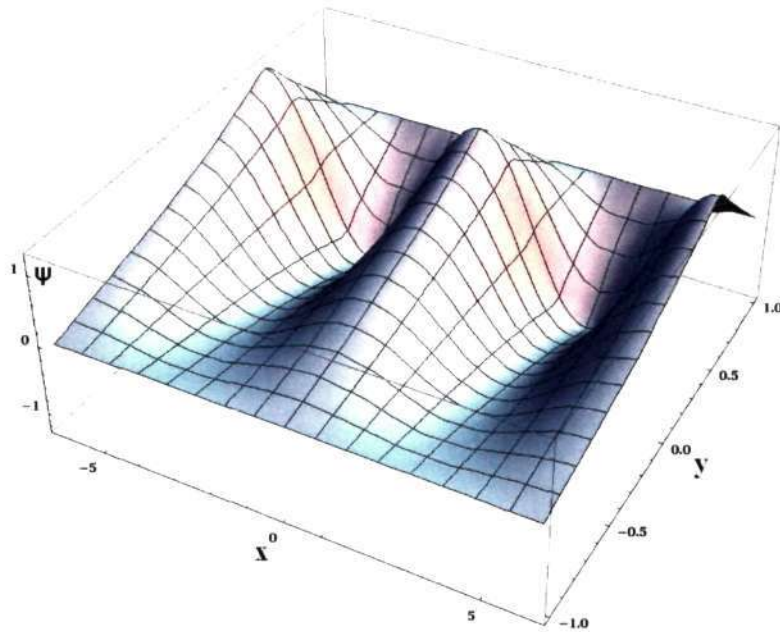


Figure 2.8: Stream function at  $t=22$  for a pure thermal perturbation.

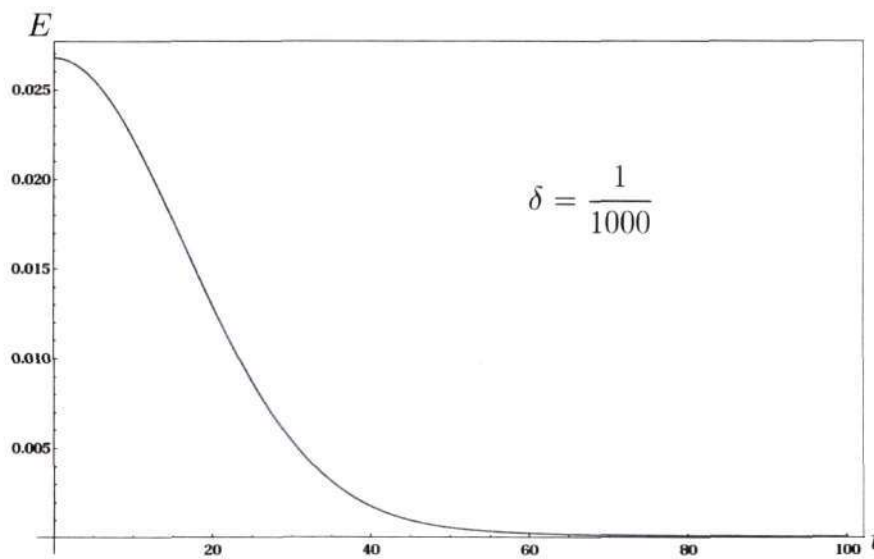
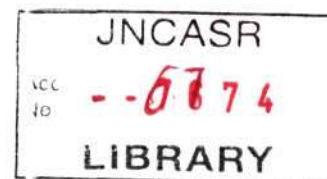


Figure 2.9: Evolution of energy due to pure vorticity perturbation, i.e. no temperature perturbation



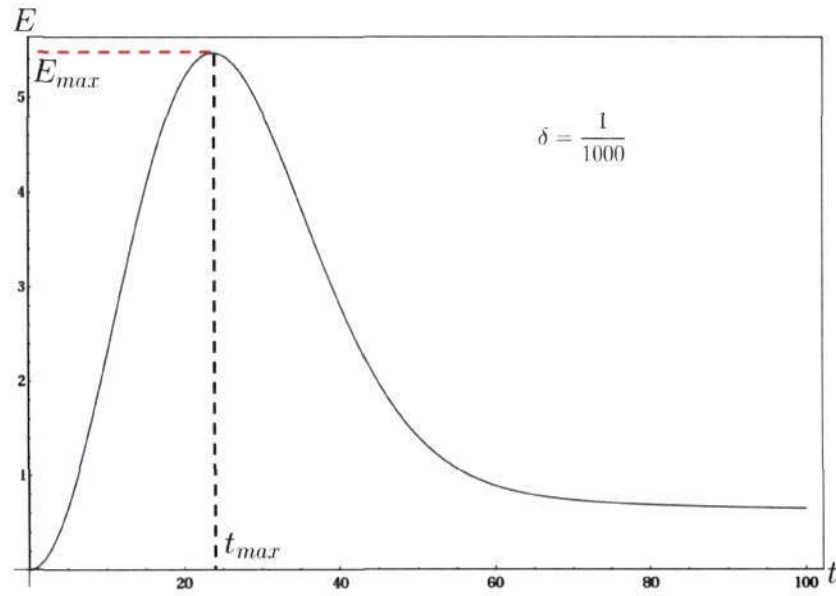


Figure 2.10: Evolution of energy due to pure temperature perturbation with no vorticity perturbation.

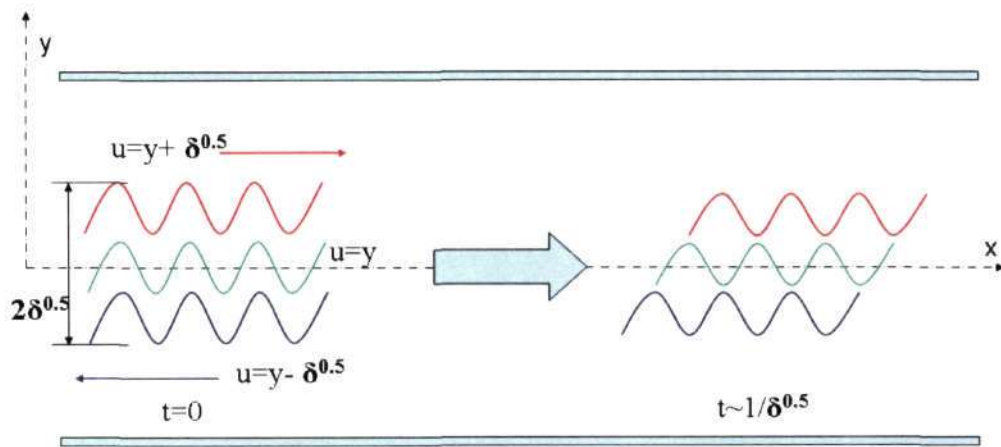


Figure 2.11: Wave Interaction

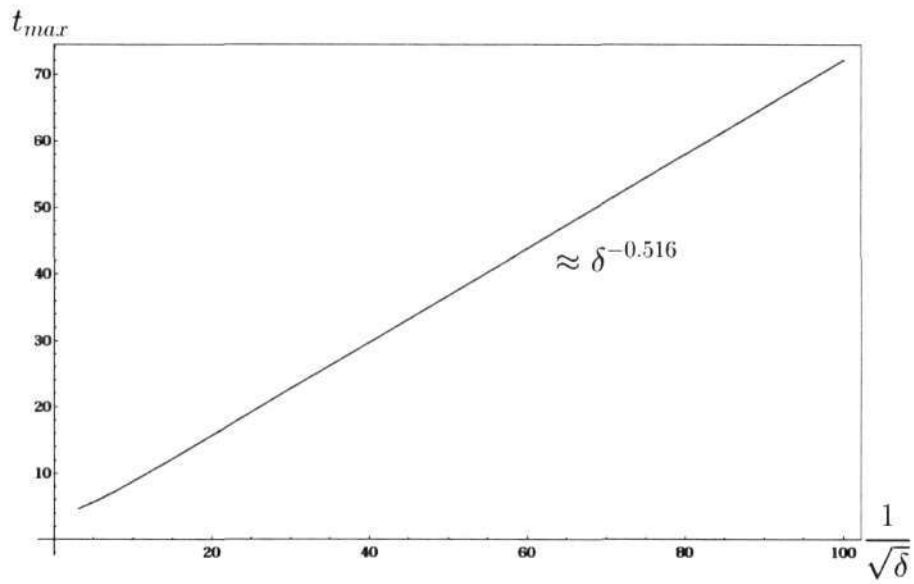


Figure 2.12: Dependence of  $t_{max}$  on the width of the Gaussian initial temperature profile.

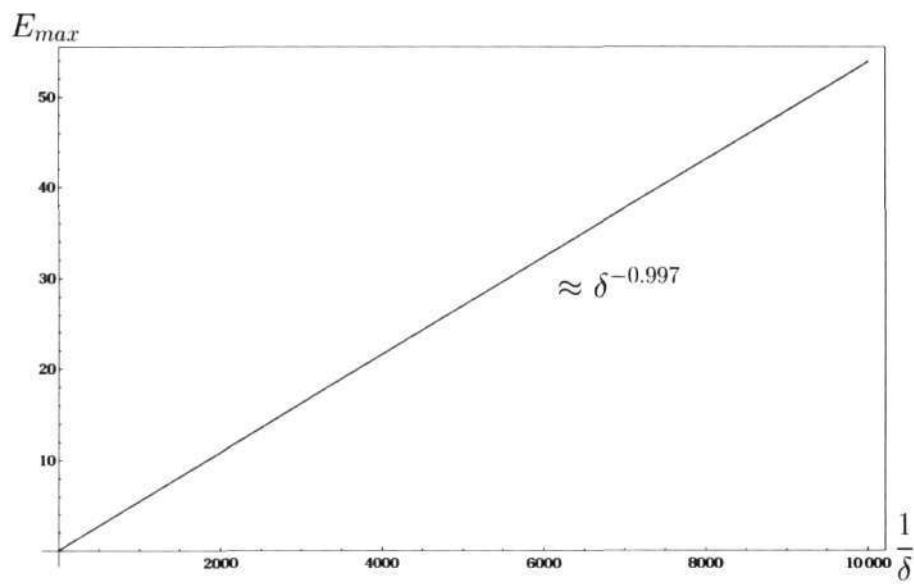


Figure 2.13: Variation of  $E_{max}$  with the width of the Gaussian initial temperature profile.

### 2.5.2 Full Inviscid problem

With the motivation from the toy problem let us move on to the full problem described by Eq (2.29). The solution of the homogeneous part of the equation is in terms of Bessel functions. If  $\hat{\psi}_1$  and  $\hat{\psi}_2$  are homogeneous solutions of the differential equation

$$\left\{ \frac{d^2}{dy^2} + a_1(y) \frac{d}{dy} + a_2(y) \right\} \hat{\psi} = 0 \quad (2.40)$$

then the corresponding Green's function is given by

$$\begin{aligned} G(y|y') &= b_1 \hat{\psi}_1(y) + b_2 \hat{\psi}_2(y) \text{ for } y < y' \\ G(y|y') &= b_1 \hat{\psi}_1(y) + b_2 \hat{\psi}_2(y) - \frac{[\hat{\psi}_1(y) \hat{\psi}_2(y') - \hat{\psi}_2(y) \hat{\psi}_1(y')]}{W(\hat{\psi}_1, \hat{\psi}_2)} \text{ for } y > y' \end{aligned} \quad (2.41)$$

where  $W(\hat{\psi}_1, \hat{\psi}_2)$  is the wronskian. The boundary conditions to be used for the greens function are  $G(y_1|y') = G(y_2|y') = 0$ , for  $y_1 = -1$  and  $y_2 = 1$ . With these boundary conditions, the greens function for stratified couette flow will be

$$\begin{aligned} G(y|y') &= \frac{\sqrt{(S +iky)(S +iky')}}{k} \\ &= \frac{(K_n(\xi_{>})I_n(\xi_{y'}) - I_n(\xi_{>})K_n(\xi_{y'}))(K_n(\xi_{<})I_n(\xi_y) - I_n(\xi_{<})K_n(\xi_y))}{K_n(\xi_1)I_n(\xi_{-1}) - K_n(\xi_{-1})I_n(\xi_1)}. \end{aligned} \quad (2.42)$$

where

$$\begin{aligned} \xi_y &= -i(S +iky) , \xi_{y'} = -i(S +iky') \\ \xi_1 &= -i(S +ik) , \xi_{-1} = -i(S -iky') \end{aligned} \quad (2.43)$$

and  $\xi_{>} = \xi_1$  &  $\xi_{<} = \xi_{-1}$  for  $y < y'$ ,  $\xi_{>} = \xi_{-1}$  &  $\xi_{<} = \xi_1$  for  $y > y'$ . With initial vorticity and temperature perturbation prescribed as forcing to the Taylor-Goldstein equation the final solution for  $\hat{\psi}$  is given by Eq (2.33). Recall that  $n = \sqrt{1/4 - Ri}$ , we are interested in stable stratification and real values of  $n$  this restricts  $Ri$  to be between 0 & 0.25 and  $n$  between 0 & 1/2. For  $Ri <$

0.25 only continuous spectra exist and singularities that occur in the integral are from inverse Laplace transform. In the contour integral in Eq (2.33) there are 2 singularities at  $S = -iky$  and  $S = -iky'$ . As before let us first study the long time behavior before addressing small time behavior. To study the asymptotic behavior of the perturbations it is sufficient to study the behavior of the region close to the singularities. Only the singularities will have contribution for  $t \gg 0$ .  $t \gg 0$  in temporal domain implies  $(S + a) \ll 1$  in the transformed domain where  $a$  is the singularity, i.e.  $S = -iky$  and  $S = -iky'$ . Let us rewrite Eq (2.33) as

$$\psi = \int_{-1}^1 [\omega_z(0)A_1 + T(0)A_2] dy' \quad (2.44)$$

where

$$\begin{aligned} A_1 &= \frac{1}{2\pi i} \int_{c-i\infty}^{c+i\infty} \frac{G(y|y')}{(S + ik y')} e^{St} dS = A_{2y} + A_{2y'} \\ A_2 &= \frac{ikRi}{2\pi i} \int_{c-i\infty}^{c+i\infty} \frac{G(y|y')}{(S + ik y')^2} e^{St} dS = A_{2y} + A_{2y'} \end{aligned} \quad (2.45)$$

where in the extreme RHS subscripts  $y$  and  $y'$  correspond to contributions due to singularities at  $y$  and  $y'$  respectively. Near the singularities  $(S + a) \ll 1$  hence the asymptotic form of the Bessel functions may be used. For small arguments the asymptotic form of the Bessel functions are

$$\begin{aligned} I_n(Z) &\sim \left(\frac{Z}{2}\right)^n \frac{1}{\Gamma(n+1)} \\ K_n(Z) &\sim \frac{\Gamma(n)}{2} \left(\frac{2}{Z}\right)^n \end{aligned} \quad (2.46)$$

We shall study the contributions from the singularities at  $S = -iky$  and  $S = -iky'$  separately.

**Contribution due to  $S = -iky$ , i.e.  $\xi_y \rightarrow 0$ .** The singularities are due to  $\sqrt{(S + ik y)} I_n(\xi_y)$  and  $\sqrt{(S + ik y)} K_n(\xi_y)$  in the inverse Laplace transform. The integrands of the two equations in Eq (2.45) can be written as

$$\begin{aligned}\frac{G(y|y')}{(S + ik y')} &\sim f_1(S)(S + ik y)^{\frac{1}{2}+n} + f_2(S)(S + ik y)^{\frac{1}{2}-n} \\ \frac{G(y|y')}{(S + ik y')^2} &\sim f_3(S)(S + ik y)^{\frac{1}{2}+n} + f_4(S)(S + ik y)^{\frac{1}{2}-n}\end{aligned}\quad (2.47)$$

Thus  $A_{1y}$  and  $A_{2y}$  can be written as

$$\begin{aligned}A_{1y} &\sim \frac{1}{2\pi i} \int f_{1,2}(s)(S + ik y)^{\frac{1}{2}\pm n} e^{St} ds \sim t^{-\frac{3}{2}\mp n} e^{-iky t} g_1(y', k) \\ A_{2y} &\sim \frac{1}{2\pi i} \int f_{3,4}(s)(S + ik y)^{\frac{1}{2}\pm n} e^{St} ds \sim t^{-\frac{3}{2}\mp n} e^{-iky t} g_2(y', k)\end{aligned}\quad (2.48)$$

where  $f_i$  are nonsingular at  $S = -iky$ ,  $g_i$  are residues of the integration. Substituting these into Eq (2.44) we get the contributions purely due to  $S = -iky$

$$\psi \sim t^{-\frac{3}{2}\pm n} e^{-iky t} \int_{-1}^1 g(y', k) dy' \quad (2.49)$$

**Contribution due to  $S = -iky'$ , i.e.  $\xi_{y'} = 0$ .** Thus singularities of principal interest are  $\sqrt{S + ik y'} I_n(\xi_{y'})$  and  $\sqrt{S + ik y'} K_n(\xi_{y'})$ . On the same lines as in case of  $S = -iky$  we get

$$A_{1y'} \sim t^{-(\frac{1}{2}\pm n)} e^{-iky' t} g_3(y, y', k) \quad (2.50)$$

$$A_{2y'} \sim t^{\frac{1}{2}\pm n} e^{-iky' t} g_4(y, y', k). \quad (2.51)$$

The decay rates of  $A_{iy}$  did not change when integrated over  $y'$  to get  $\psi$  as  $y'$  was not coupled with time-dependent terms. But in  $A_{iy'}$   $y'$  is coupled with the time-dependent term, thus the decay rates due to  $A_{iy'}$  have changed when integrated over  $y'$  to get  $\psi$ . As in the toy problem we shall examine response to initial conditions in vorticity and temperature which are  $\delta$  functions located at  $y = y_1$ . Corresponding to initial conditions in Eq (2.36) decay rates of  $A_{iy}$  and  $A_{iy'}$  will remain same on integration to obtain  $\psi$ . Remember that  $0 < n < 1/2$  for stable stratification with  $Ri < 1/4$ , for this range of  $n$   $\psi$  would experience a decay in time, for both vorticity and temperature initial condition due to  $A_{iy}$ .  $\tilde{\psi}$  would



also experience decay for a vorticity initial condition corresponding to  $A_{1y'}$ , but it would experience a sublinear growth in  $t$ , going as  $t^{n+1/2}$ , for the temperature initial condition corresponding to  $A_{2y'}$ . Thus for a singular initial condition in thermal perturbation one would observe growth in time at all times.

It is clear that a singular initial condition in thermal perturbation leads to unbounded growth, but would a smooth initial condition in vorticity and thermal perturbation lead to such a growth? Since time dependence in  $A_{iy}$  is not combined with  $y'$  a smooth initial condition, either in vorticity or temperature, would not change the asymptotic behavior. The difference comes from  $A_{iy'}$  where time dependence is coupled with  $y'$ , the response to a smooth initial condition would be very different from that to a delta initial condition. As we have seen growth occurs only due to  $A_{2y'}$ . Considering only smooth thermal perturbation, we have

$$\psi \sim \int_{-1}^1 \tilde{T}(0) A_{2y'} dy'. \quad (2.52)$$

It was shown for the toy problem the integral would lead to a  $O(1/t^2)$  decay.

$$\int_{-1}^1 e^{-iky't} G_4(y, y', k) \sim O\left(\frac{1}{t^2}\right) \quad (2.53)$$

Thus at large time

$$\psi \sim t^{\frac{1}{2} \pm n} t^{-2} e^{-iky't} \sim t^{-\frac{3}{2} \pm n} e^{-iky't} \quad (2.54)$$

Hence, for a smooth initial condition the contribution from  $S = -iky'$  will lead to  $t^{-\frac{3}{2} \pm n}$  decay as  $S = -iky$  did. We saw in the toy problem that there is a decay for smooth initial condition but a growth for delta initial condition, it was shown that at short times there will be a growth for smooth initial condition before the asymptotic decay. In the full problem  $A_{1y}$ ,  $A_{2y}$  and  $A_{1y'}$  all decay when excited by a delta function. Only  $A_{2y'}$  grows as  $t^{n+1/2}$ . For a smooth initial condition the first three show the same leading order decay for  $t \gg 0$ . But short time  $A_{2y'}$  first grows before the asymptotic decay.



## CHAPTER 3

# TRANSIENT GROWTH IN VISCOUS STRATIFIED SHEAR FLOW

In the current chapter we consider viscous shear flow with stratification. Density as well as viscosity stratification are addressed in this chapter, their individual effects and their combined effects are studied. Two different flows are considered, Couette and Poiseuille flow. We study the effect of stratification on the transient growth of the flow, find that in some cases there is a slight change in the qualitative nature of transient growth in Couette flow. We study the effect of Prandtl and Grashof number on the transient growth and its nature.

### 3.1 Linear Stability

In Chapter 2 the linearized stability equations for a density stratified parallel flow were derived, in this chapter we consider viscosity stratification along with density stratification. To derive the stability equations we have to go back to the Navier-Stokes equation which remains unchanged except for the diffusion term.

$$\frac{DU}{Dt} = -\frac{1}{\rho}\nabla P + \nabla\nu(y)\nabla U - i_{\mathbf{y}}\frac{g\alpha_T\Delta T}{\rho} \quad (3.1)$$

Let us consider only the diffusion term, writing only the diffusion term in index notation for simplicity as

$$\partial_i(\mu(\partial_j U_i + \partial_i U_j)) \quad (3.2)$$

with  $U$  and  $\mu$  in terms of mean and perturbation as

$$\begin{aligned} U &= \bar{U} + u \\ \mu &= \bar{\mu} + \hat{\mu} \end{aligned} \quad (3.3)$$

Substituting these into Eq (3.2), subtracting the resulting equation with the corresponding equation for mean quantities and neglecting nonlinear terms we get the diffusion terms in the perturbation equation.

$$\partial_j \mu (\partial_j u_i + \partial_i u_j) + \partial_j \hat{\mu} (\partial_j U_i + \partial_i U_j) + \mu \partial_j \partial_j u_i + \hat{\mu} \partial_j \partial_j U_i \quad (3.4)$$

In the above equations the over bars for mean quantities have been neglected. Substitute components of the above equation in Eq (2.1)- (2.3) and following the same procedure as in section 2.1 of Chapter 2 we arrive at the linearized perturbation equations. The resulting equations are in terms of perturbation viscosity, but stratification is expressed in terms of the temperature perturbation equation hence we express perturbation viscosity in terms of thermal perturbation. Writing viscosity as  $\mu = \bar{\mu} + \hat{\mu} = f(\bar{T}, T)$ , and using Eq (3.3)

$$\begin{aligned} \mu &= \bar{\mu} + \frac{\partial \bar{\mu}}{\partial \bar{T}} T \text{ thus} \\ \hat{\mu} &= \frac{\partial \bar{\mu}}{\partial \bar{T}} T \end{aligned} \quad (3.5)$$

The Arrhenius model is used to describe the dependance of mean viscosity on temperature. Temperature variation is only along  $y$  thus viscosity will be a function of  $y$  only,  $\mu = \mu(y)$ . The model used is

$$\mu_d(\bar{T}) = C_1 \exp(C_2/\bar{T}) \quad (3.6)$$

where  $\mu_d$ , dynamic viscosity, is in dimensional from,  $C_1, C_2$  are constants and the values assumes are for water,  $C_1 = 0.00183 Nsm^{-2}$  and  $c_2 = 1879.9 K$  (see, e.g., Sameen and Govindarajan 2007). As mean viscosity is a function of temperature its normal derivative can be expressed in terms of normal derivative of mean temperature.

$$\frac{\partial \mu}{\partial y} = \frac{\partial \mu}{\partial \bar{T}} \frac{\partial \bar{T}}{\partial y} \quad (3.7)$$

Similarly the higher derivative of  $\mu$  with respect to  $y$  can be expressed in terms of normal derivative of mean temperature. Thus writing mean and perturbation viscosity and their derivatives in terms of mean and perturbation temperature

and their derivatives respectively we get the stability equations for perturbation temperature, wall normal perturbation velocity and spanwise vorticity same as Sameen and Govindarajan(2007).

$$\begin{aligned}
& [(-i\alpha c + i\alpha U)(D^2 - k^2) - i\alpha U'']v = \frac{1}{Re} [\mu(D^2 - k^2)v + \frac{\partial\mu}{\partial T}\bar{T}'[2(D^3 - k^2D)v] \\
& + \frac{\partial\mu}{\partial T}\bar{T}''[(D^2 + k^2)v] + \frac{\partial^2\mu}{\partial^2 T}(\bar{T}')^2[D^2 + k^2]v \\
& - i\alpha[\frac{\partial\mu}{\partial T}(U'D^2 + 2U''D + (U''' + \alpha^2U'))T + \frac{\partial^2\mu}{\partial^2 T}(2\bar{U}'\bar{T}'D + 2\bar{U}''\bar{T}' + \bar{T}''\bar{U}')T \\
& + \frac{\partial^3\mu}{\partial^3 T}\bar{T}'^2\bar{U}'T]] + k^2\frac{Gr}{Re^2}T, \tag{3.8}
\end{aligned}$$

$$\begin{aligned}
(-i\alpha c + i\alpha U)\eta + i\beta\bar{U}'V &= \frac{1}{Re} [((D^2 - K^2) + \frac{\partial\bar{\mu}}{\partial T}\bar{T}'D)\eta \\
& + (i\beta\frac{\partial\bar{\mu}}{\partial T}\bar{U}'D + i\beta\frac{\partial^2\bar{\mu}}{\partial^2 T}\bar{T}'U' + i\beta U''\frac{\partial\mu}{\partial T})T], \tag{3.9}
\end{aligned}$$

$$(-i\alpha c + i\alpha U)T + \bar{T}'v = \frac{1}{RePr}(D^2 - k^2)T \tag{3.10}$$

where  $\mu = \mu_d/\mu_{ref}$  is the dimensionless viscosity,  $\mu_{ref}$  is the reference viscosity(reference taken at hot wall in Couette and Poiseuille flow). As viscosity varies along y the Reynolds number is defined in terms of average viscosity

$$Re = \frac{U_{max}\rho h}{\frac{1}{2}\int_{-1}^1 \mu_d dy}. \tag{3.11}$$

The above set of equations can be written as an initial value problem in a compact form as

$$\begin{pmatrix} (D^2 - k^2) & 0 & 0 \\ 0 & 1 & 0 \\ 0 & 0 & 1 \end{pmatrix} \frac{\partial}{\partial t} \begin{pmatrix} v \\ \eta \\ T \end{pmatrix} + \begin{pmatrix} L_{OS} & 0 & k^2 Ri + L_{OST} \\ -i\beta U & L_{SQ} & L_{ST} \\ T' & 0 & L_T \end{pmatrix} \begin{pmatrix} v \\ \eta \\ T \end{pmatrix} \tag{3.12}$$

The operators in the above equation are

$$L_{OS} = (i\alpha U)(D^2 - k^2) - i\alpha U'' - \frac{1}{Re}[\mu(D^2 - k^2) + \frac{\partial\mu}{\partial T}\bar{T}'2(D^3 - k^2D) + \frac{\partial\mu}{\partial T}\bar{T}''(D^2 + k^2) + \frac{\partial^2\mu}{\partial^2 T}(\bar{T}')^2(D^2 + k^2)] \quad (3.13)$$

$$L_{OST} = -\frac{i\alpha}{Re}[\frac{\partial\mu}{\partial T}(U'D^2 + 2U''D + (U''' + \alpha^2U')) + \frac{\partial^2\mu}{\partial^2 T}(2\bar{U}'\bar{T}'D + 2\bar{U}''\bar{T}' + \bar{T}''\bar{U}')] + \frac{\partial^3\mu}{\partial^3 T}\bar{T}'^2\bar{U}' \quad (3.14)$$

$$L_{SQ} = (i\alpha U) - \frac{1}{Re}[(D^2 - k^2) + \frac{\partial\bar{\mu}}{\partial T}\bar{T}'D] \quad (3.15)$$

$$L_{ST} = \frac{1}{Re}[i\beta\frac{\partial\bar{\mu}}{\partial T}\bar{U}'D + i\beta\frac{\partial^2\bar{\mu}}{\partial^2 T}\bar{T}'U' + i\beta U''\frac{\partial\mu}{\partial T}] \quad (3.16)$$

$$L_T = i\alpha U - \frac{1}{RePr}(D^2 - k^2) \quad (3.17)$$

The initial value problem in Eq (3.12) can be written in a simplified form as

$$M\frac{\partial}{\partial t}x = Lx \longrightarrow \frac{\partial}{\partial t}x = M^{-1}Lx = \mathcal{A}\xi \quad (3.18)$$

where  $x = (v, \eta, T)^T$ , comparing Eq (3.18) and Eq (3.12) we can clearly see what M and L correspond to.

## 3.2 Transient Growth

We wish to study the temporal evolution of perturbations to look for transient growth in their energy. Treating the linear stability equation as an initial value problem will give evolution of perturbations for random initial conditions. The initial condition used may not lead to the maximum possible growth, but we need to study the worst possible initial condition which leads to maximum growth of the perturbation energy. Thus we turn to transient growth analysis to study evolution of perturbation energy due to optimal initial conditions which lead to maximum growth. We use the same technique used by Reddy & Henningson(1993) and Schmid & Henningson(2001).

Let  $\omega_i$  and  $\bar{x}_i$  be the eigenvalues and eigenvectors of  $\mathcal{A}$  respectively and let  $S_N$  be the span of N eigenvectors of  $\mathcal{A}$  corresponding to first N least stable eigenvalues.

$$S_N = \langle \tilde{x}_1, \tilde{x}_2, \tilde{x}_3, \dots, \tilde{x}_N \rangle \quad (3.19)$$

Writing the vector perturbation in terms of a linear combination of eigenvectors  $x_i$

$$x(y, t) = \sum_{i=1}^N \kappa_i(t) \tilde{x}_i \quad (3.20)$$

where  $\kappa_i$  is the  $i^{\text{th}}$  expansion coefficient of the eigenvectors. Thus with the above expansion we can write the initial value problem in Eq (3.18) in terms of the expansion coefficients as

$$\frac{d\kappa}{dt} = -i\Lambda\kappa \quad (3.21)$$

where  $\kappa = (\kappa_1, \kappa_2, \kappa_3, \dots, \kappa_N)^T$  and  $\Lambda = \text{diag}(\omega_1, \omega_2, \omega_3, \dots, \omega_N)$ .

The 2-norm, in terms of inner product, is defined as

$$\|x\|_2 = (x_1, x_2)_2 = \frac{1}{k^2} \int_{-1}^1 x_2^\dagger x_1 dy = \kappa_2^\dagger \kappa_1 \quad (3.22)$$

where  $\dagger$  implies hermitian, conjugate transpose. With the above definition of 2 norm we can define the energy norm in terms as

$$\|x\|_E = \frac{1}{k^2} \int_{-1}^1 x_2^\dagger W x_1 dy = \kappa_2^\dagger w \kappa_1 \quad (3.23)$$

where  $W$  is called the weight matrix which is problem specific. If we factorize  $W$  as  $W = F^\dagger F$  (and  $w = f^\dagger f$ ) then we can energy norm in terms of the inner product

$$(x_1, x_2)_E = (F x_1, F x_2)_2 = (f \kappa_1, f \kappa_2)_2 \quad (3.24)$$

The perturbation energy is the sum of the disturbance kinetic and potential energy which is defined as (Hanifi, Schmid & Henningson(1996), Saneen & Govindarajan(2007))

$$E = \frac{1}{2} \int (|u|^2 + |v|^2 + |w|^2 + B|T|^2) dy \quad (3.25)$$

In terms of wall normal velocity, spanwise vorticity and temperature, the energy can be rewritten as

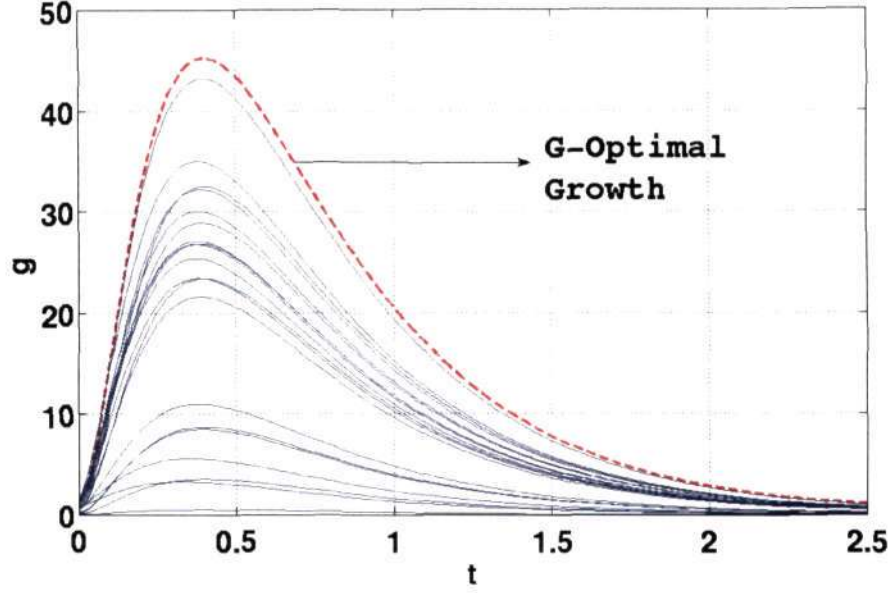


Figure 3.1: Evolution of  $g$  for random initial conditions

$$E = \int (|Dv|^2 + k^2|v|^2 + |\eta|^2 + B|T|^2)dy \quad (3.26)$$

In all our computation we choose  $B$  to be 1. From which we can see that the associated weight matrix appearing in the definition of energy norm is

$$W = \begin{pmatrix} D^2 + k^2 & 0 & 0 \\ 0 & 1 & 0 \\ 0 & 0 & 1 \end{pmatrix}. \quad (3.27)$$

Defining a growth parameter similar to what was defined in Chapter 1

$$g(t, \alpha, \beta) = \frac{\|x(t)\|_E^2}{\|x(0)\|_E^2} = \frac{\|\kappa(t)\|_E^2}{\|\kappa(0)\|_E^2} \quad (3.28)$$

The optimal growth is one which is maximized over all initial conditions and  $G_{max}$  is as defined in Eq (1.10).



$$\begin{aligned}
G(t, \alpha, \beta) &= \max_{\kappa(0) \neq 0} \frac{\|\kappa(t)\|_E^2}{\|\kappa(0)\|_E^2} = \max_{\kappa(0) \neq 0} \frac{\|e^{-i\Lambda t} \kappa(0)\|_E^2}{\|\kappa(0)\|_E^2} \\
&= \max_{\kappa(0) \neq 0} \frac{\|f e^{-i\Lambda t} \kappa(0)\|_2^2}{\|f \kappa(0)\|_2^2} \\
G(t, \alpha, \beta) &= \|f e^{-i\Lambda t} f^{-1}\|_2^2
\end{aligned} \tag{3.29}$$

$g$  in Eq(3.28) gives the evolution of normalized perturbation energy for a given initial condition, for different initial condition  $g$  will evolve differently. In a plot of  $g$  vs  $t$  there will be various curves corresponding to various initial conditions. If we manage to span over all possible initial conditions, then the initial condition which yields a curve that envelopes all other curves is the optimal initial condition and this curve is given by  $G$  and the peak of this curve is given by  $G_{max}$ . Fig 3.1 shows the evolution of  $g$  an arbitrary initial value problem, the red dashed line, which envelopes all the other curves, is the optimal growth of  $g$ .

### 3.3 Couette Flow

In this section we will be dealing with Couette flow with only density stratification, i.e. constant viscosity. With  $U'' = 0$  and only density stratification Eq (3.8)-(3.10) reduce to

$$[(-i\alpha c + i\alpha U)(D^2 - k^2)]v = \frac{1}{Re}(D^2 - k^2)v + RiT \tag{3.30}$$

$$(-i\alpha c + i\alpha U)\eta + i\beta v = \frac{1}{Re}(D^2 - K^2)\eta \tag{3.31}$$

$$(-i\alpha c + i\alpha U)T + \bar{T}'v = \frac{1}{RePr}(D^2 - k^2)T \tag{3.32}$$

#### 3.3.1 Stable Stratification

The stably stratified Couette flow in 2D (bounded and unbounded) has been studied in literature, but it was not until early 1990 that the transient growth aspect of the problem was looked at. Farrel & Ioannou (1993) found that for a stably

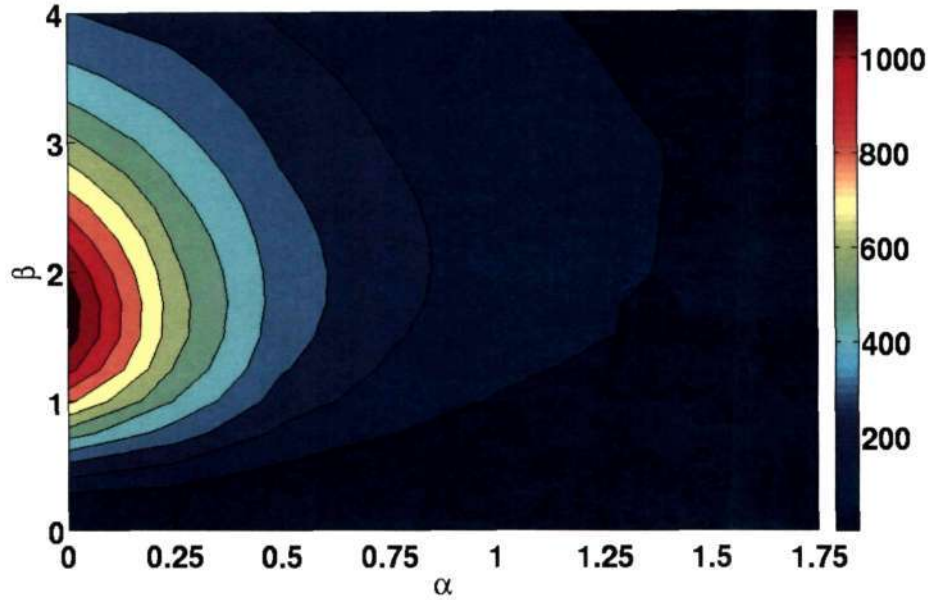


Figure 3.2:  $G_{max}$  contours for plane Couette flow without stratification.

stratified inviscid 2D bounded Couette flow the transient growth decreases with increasing stratification. In our analysis of a 3D viscous Couette flow we find something similar.

We present the contours of  $G_{max}$ , i.e. maximum of  $G$  over all time in the  $\alpha - \beta$  plane, all the results are for a fixed Reynold's number of 1000, and for a temperature gradient of  $25^0K$ . The two other non-dimensional numbers, Prandtl and Grashof, are varied. The results for different Grashof numbers implies results for different levels of buoyancy and variation of Prandtl number implies that the fluid upon which the analysis is made is being changed.

In Fig. 3.2 the  $G_{max}$  contours of a plane Couette flow are shown. At  $Gr = 10$  and  $Pr = 10^{-4}$  there isn't any, quantitative or qualitative, change in the contour of  $G_{max}$ . But if we increase the Prandtl, effectively changing the fluid, keeping Grashof a constant at 10 we find that the maximum transient growth on  $\alpha - \beta$  plane increases. The max growth increases from around 1100 to 1400 when Pr in increased from  $10^{-4}$  to 1 which is shown in Fig 3.3-3.5.

The results become more interesting when the Grashof is changed keeping the Prandtl fixed. At low levels of buoyancy(Grashof) note that the maximum growth occurs at  $\alpha = 0$  and between  $\beta = 1.5 - 2$ , i.e the maximum growth occurs when the

perturbation waves have purely spanwise dependence and no streamwise dependence. When the Grashof is increased from 10 to 10000 through 1000 for Prandtl of 0.1 we find a qualitative change in the result, this can be seen in Fig 3.4 ,3.6 and Fig 3.7. The max growth which occurred at  $\alpha = 0$  now occurs at non-zero  $\alpha$ . The other change is quantitative, the maximum growth decreases when Grashof is increased as can be seen in the above mentioned figures and this is analogous to the results of Farrel & Ioannou (1993). With  $Gr = 100000$  when Pr is increased from 0.1 to 1 the max growth does not increase but the location of maximum growth in the  $\alpha - \beta$  plane shifts to right by a small amount. The dominant structure in the flow are thus expected to be suppressed in strength and are at an inclination different from the streamwise streaks.

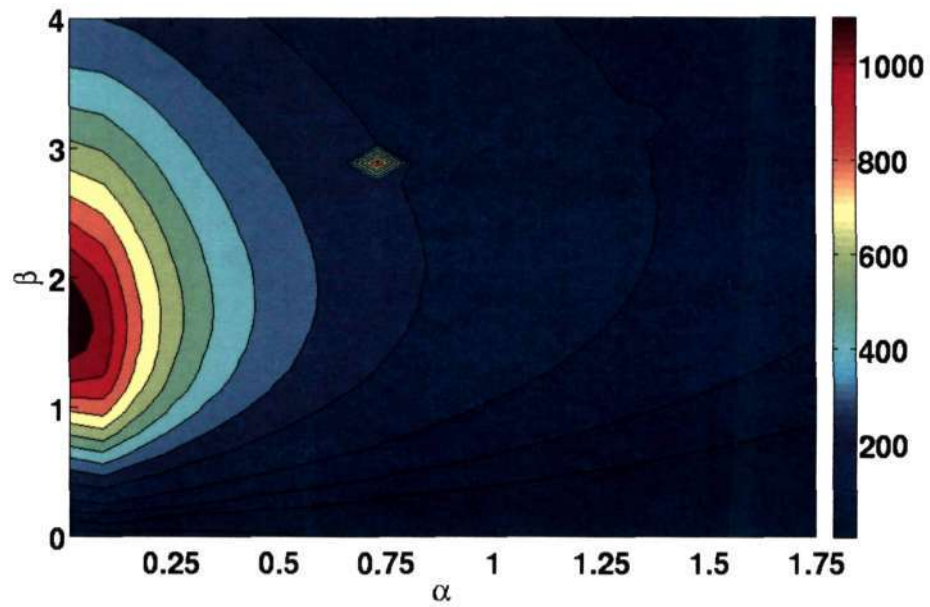


Figure 3.3:  $G_{max}$  contours with stratification,  $Gr = 10$ ,  $Pr = 10^{-4}$ .

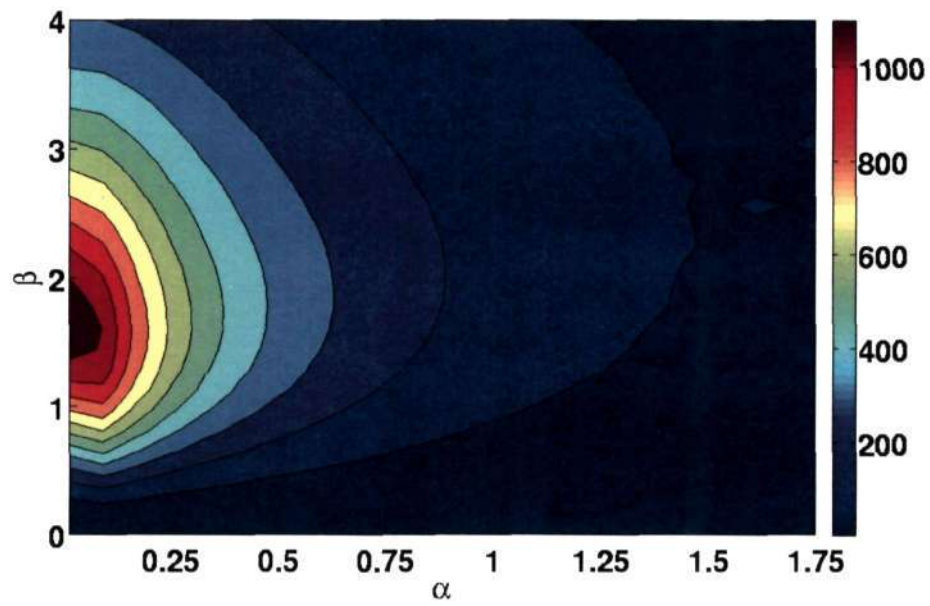
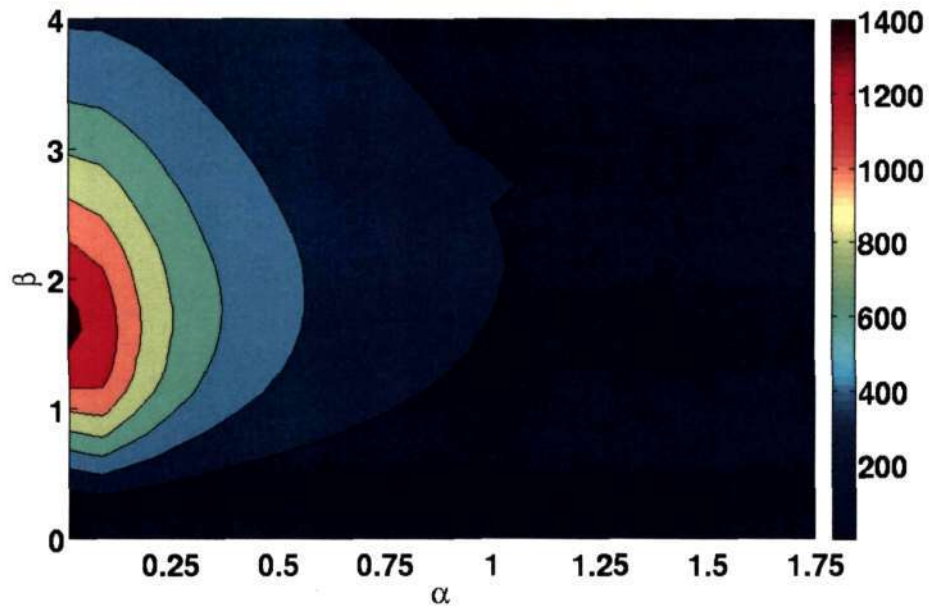
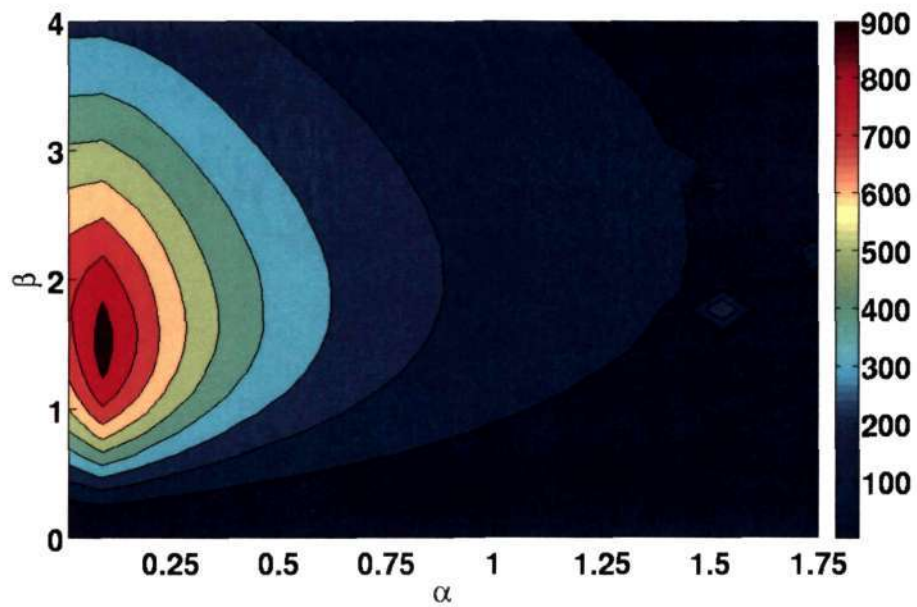
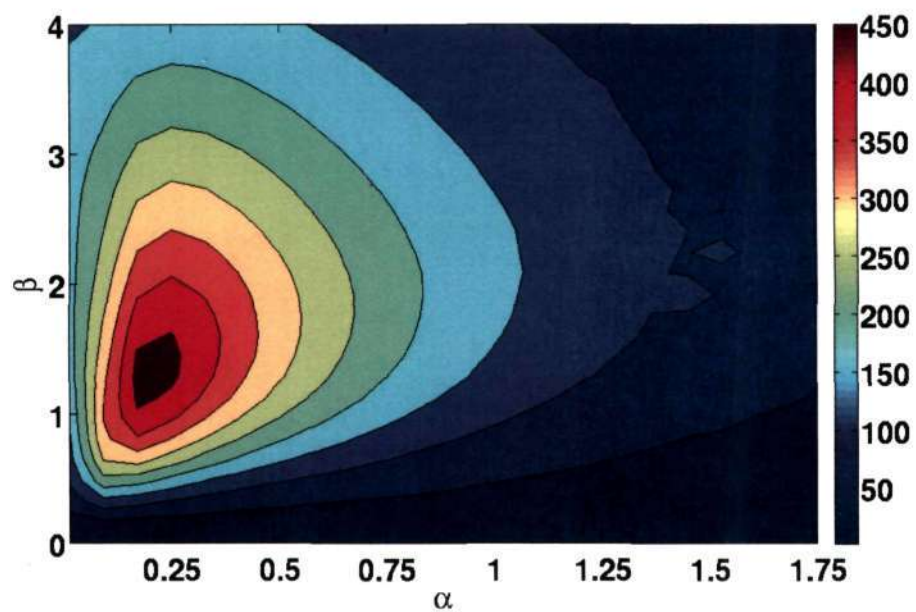
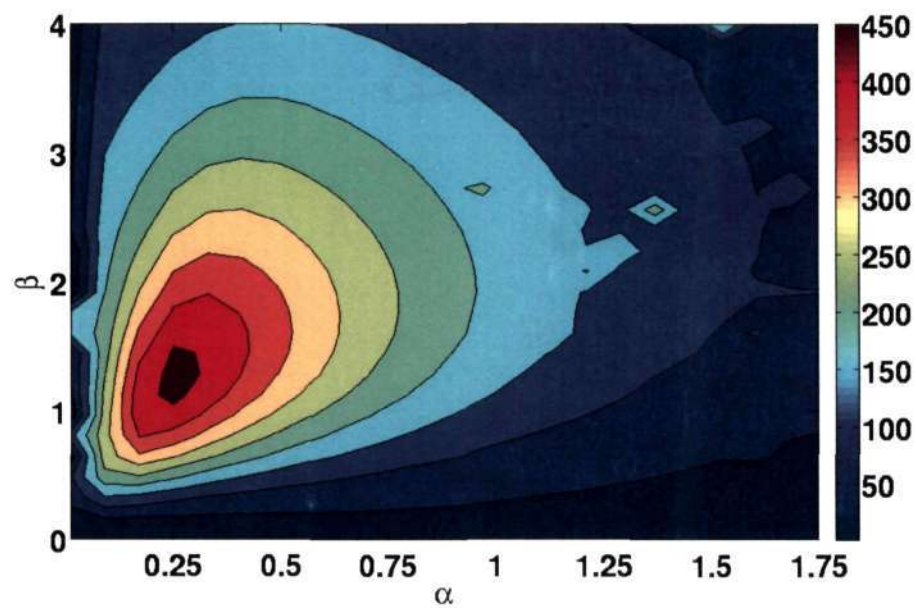


Figure 3.4: Same as Fig: 3.3 but  $Pr = 10^{-1}$

Figure 3.5: Same as Fig: 3.3 but  $Pr = 1$ Figure 3.6: Increased Richardson number with  $Gr = 1000$  &  $Pr = 10^{-1}$

Figure 3.7:  $Gr=10000$   $Pr = 10^{-1}$ Figure 3.8:  $Gr=10000$   $Pr = 1$

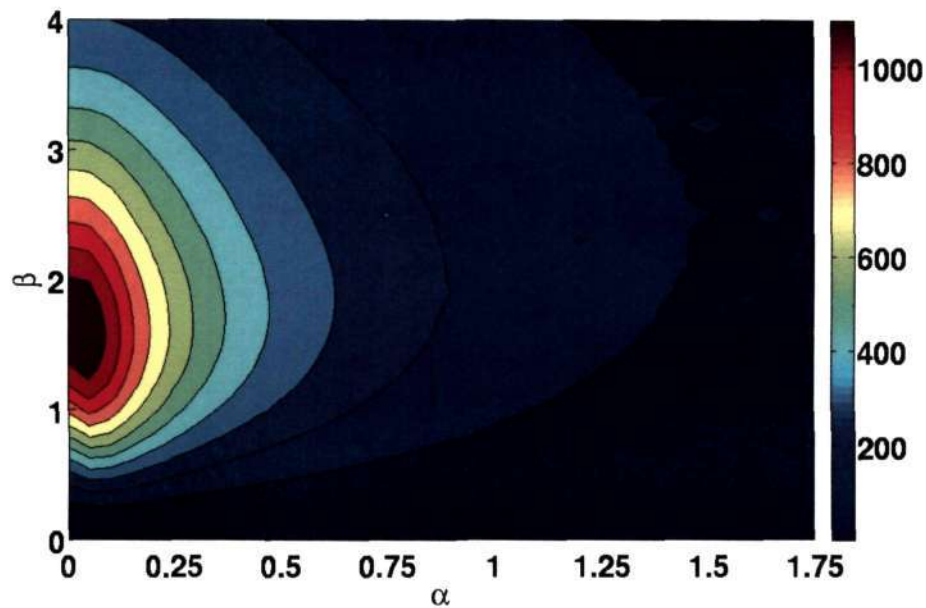


Figure 3.9:  $Gr = -10$ ,  $Pr = 0.1$ , Transient growth does not change at small  $Gr$  and small  $Pr$

### 3.3.2 Unstable Stratification

Unstable stratification has an adverse effect on the linear stability of the flow, it has a similar effect on the transient growth as well. At small values of Grashof number increasing Prandtl number does not have any effect on the transient growth upto a Prandtl of 0.1 beyond which there is an increase in transient growth. In Fig 3.9 we see that the  $G_{max}$  contours are similar to ones of plane Couette flow, in Fig 3.10 we see that there is an increase in transient growth when Prandtl number is increased to 1. Increasing buoyancy does not have the same effect as in stable stratification, on the contrary there is an increase in the transient growth and  $\alpha$  dependance of maximum  $G_{max}$  does not change much. Increasing buoyancy also leads to linear instability and the  $Gr$  at which the linear instability occurs reduces with increasing Prandtl number. From Fig 3.11 it can be seen that the transient growth has increased when  $Gr$  is increased to -1000.

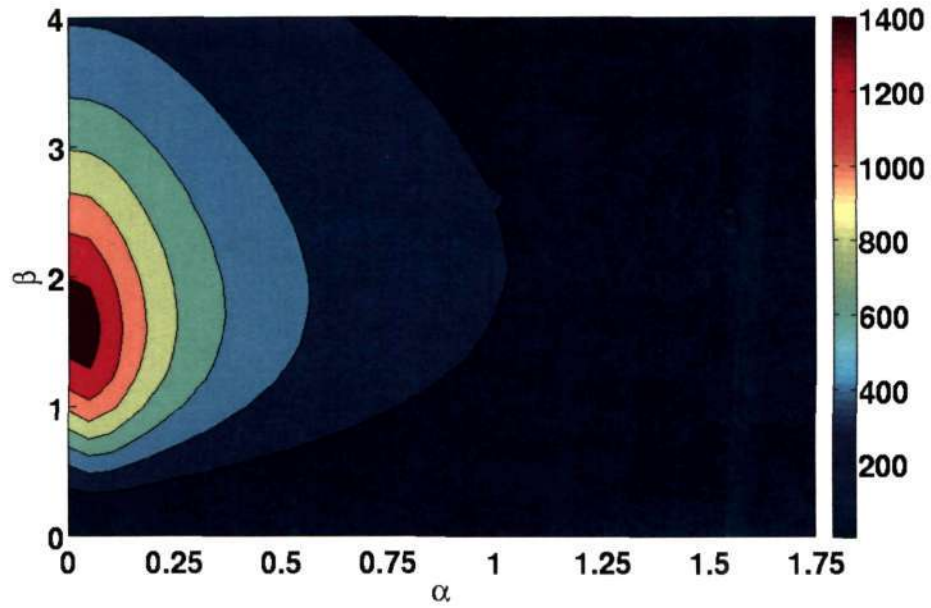


Figure 3.10:  $Gr = -10$ ,  $Pr = 1$ , Transient growth increase when  $Pr$  is increased

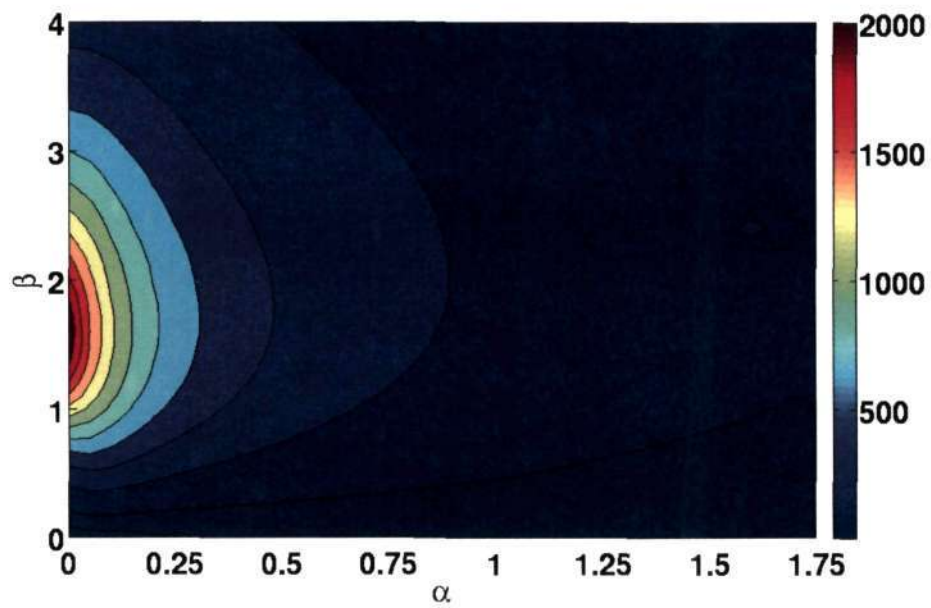


Figure 3.11: There is an increase in transient growth with increase in  $Gr$ ,  $Gr = -1000$  &  $Pr = 0.1$



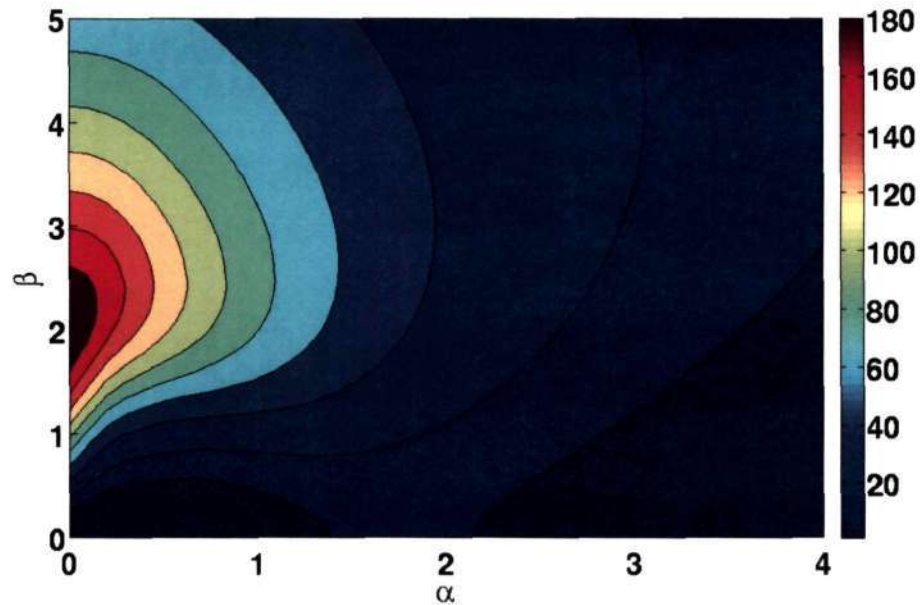


Figure 3.12:  $G_{max}$  contours of unheated Poiseuille flow

### 3.4 Poiseuille Flow - Density Stratification

In case of no viscosity stratification the only change to the Orr-Sommerfeld equation is addition of the temperature perturbation coupling term. The governing equations are same as Eq (3.30)-(3.32) except that  $U'' \neq 0$  hence Eq (3.30) changes to

$$[(-i\alpha c + i\alpha U)(D^2 - k^2) - i\alpha U'']v = \frac{1}{Re}(D^2 - k^2)v + RiT \quad (3.33)$$

The nature and trend of the transient growth solutions of Poiseuille flow with density stratification is the same as Couette flow with density stratification both for stable and unstable stratification.

#### 3.4.1 Stable Stratification

As in case of density stratified Couette flow effect of increasing the Prandtl number is to increase the maximum transient growth although stratification is stable. Fig 3.12 shows the  $G_{max}$  contours for plane unheated Poiseuille flow case, adding heat with a small Gr of 1 and a small Pr of 0.001 hardly changes the contours of  $G_{max}$ , as can be seen in Fig 3.13. But from Fig 3.14 it can be seen that if Pr is increased then

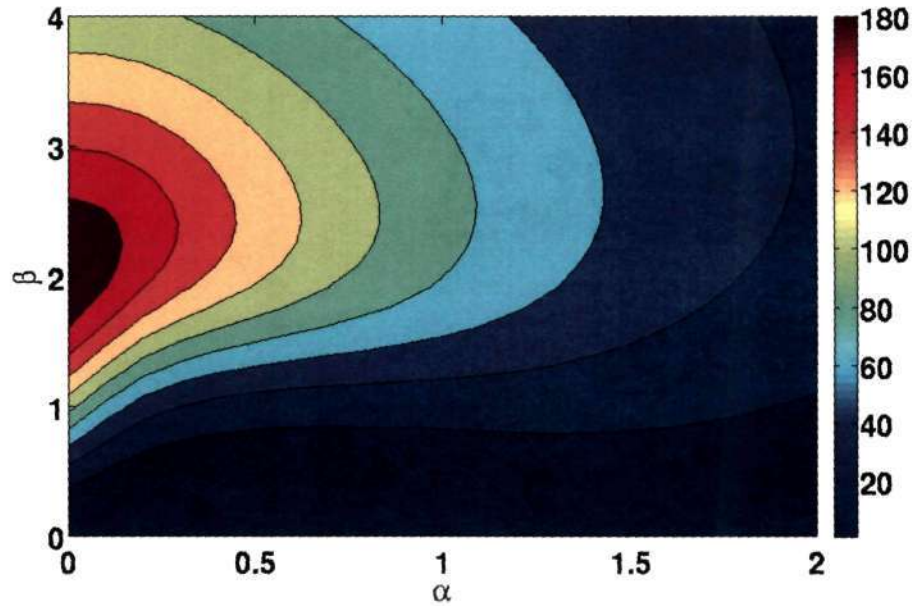


Figure 3.13:  $Gr = 1$  and  $Pr = 10^{-3}$ , there is hardly any change in the transient growth from the unheated case.

there is an increase in the transient growth. The effect of buoyancy is to reduce the maximum transient growth. Keeping  $Pr$  at 1 if we increase the buoyancy we can notice two effects, one is a reduction in the transient growth and the other is to increase the streamwise dependence of perturbation waves which cause maximum transient growth. In Fig 3.15 we can see that the maximum transient growth has reduced and the region of maximum transient growth has extended to the right of  $\alpha - \beta$  plane up to  $\alpha = 0.41$ . On further increasing  $Gr$  the region of maximum growth detaches from the  $\beta$  axis and the maximum growth is reduced even more which is shown in Fig 3.16.

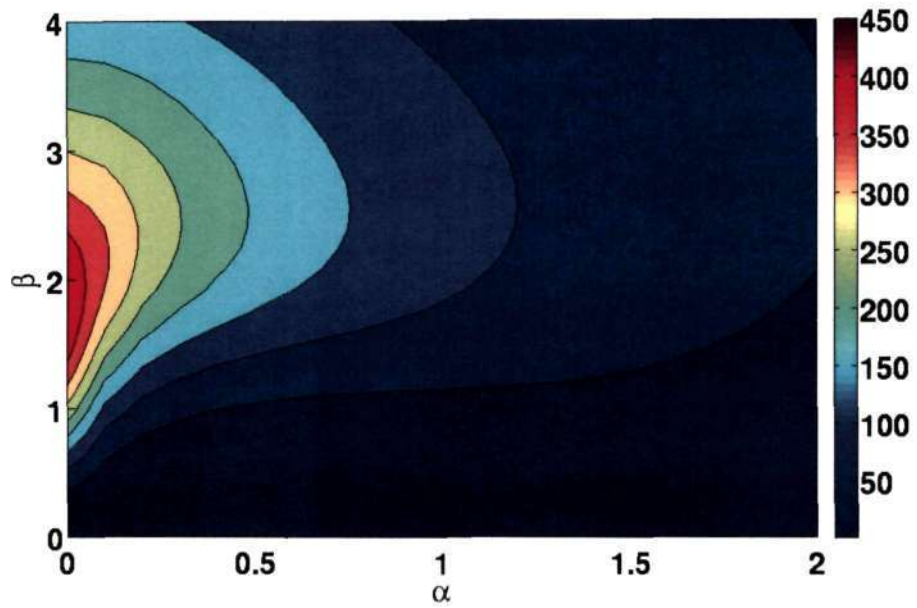


Figure 3.14: Stably Stratified Poiseuille flow with  $Gr = 1$  and  $Pr = 1$ .

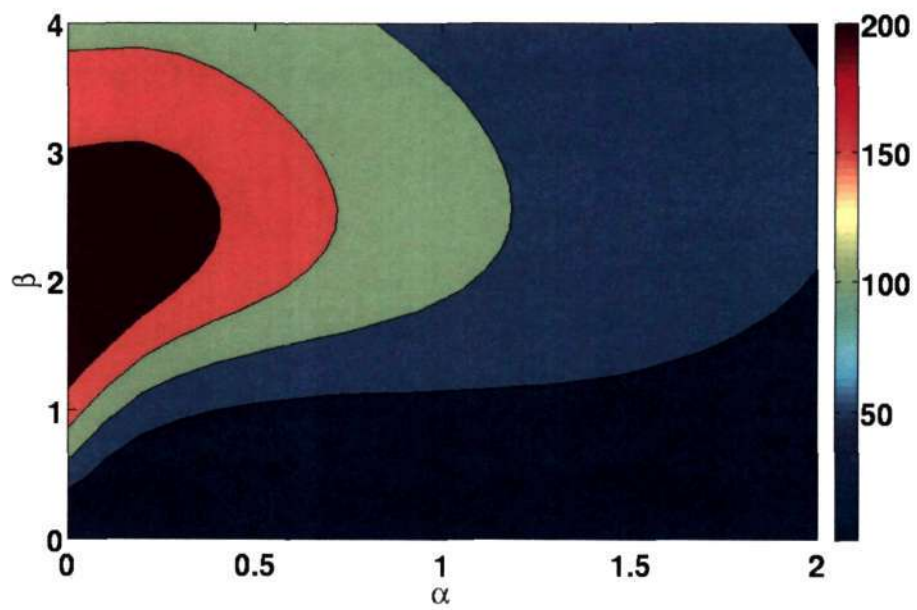


Figure 3.15: In stable stratification Increasing Buoyancy seems to decrease transient growth,  $Gr = 1000$  and  $Pr = 1$ .

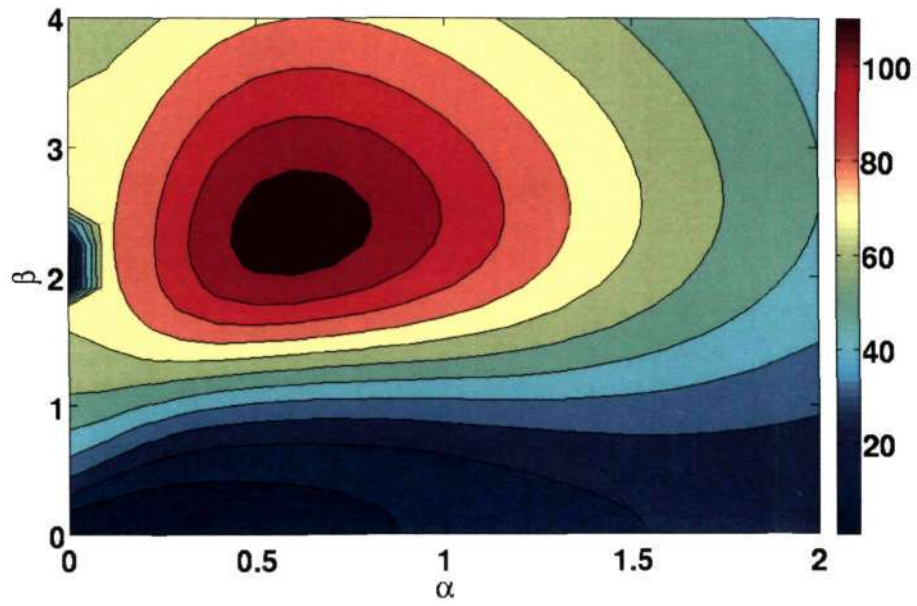


Figure 3.16: The Transient growth is reduced even more with increase in Buoyancy,  $Gr = 10000$  and  $Pr = 1$ .

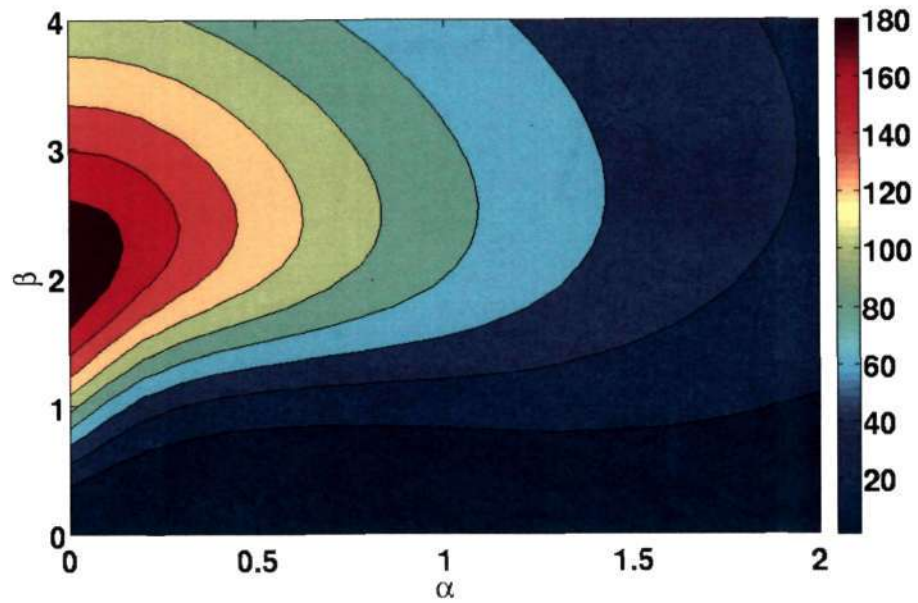


Figure 3.17: Unstable stratification with  $Gr = -1$ ,  $Pr = 10^{-3}$ .

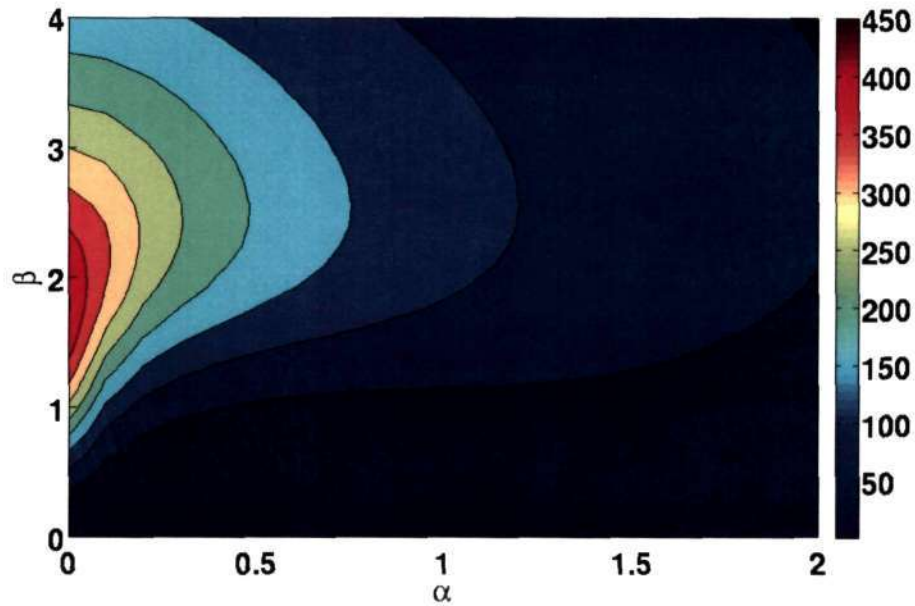
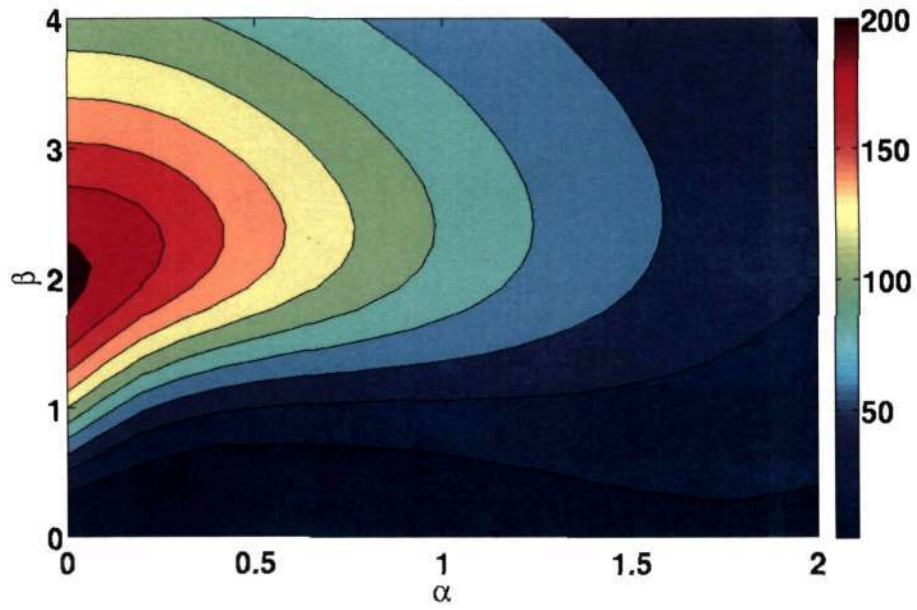
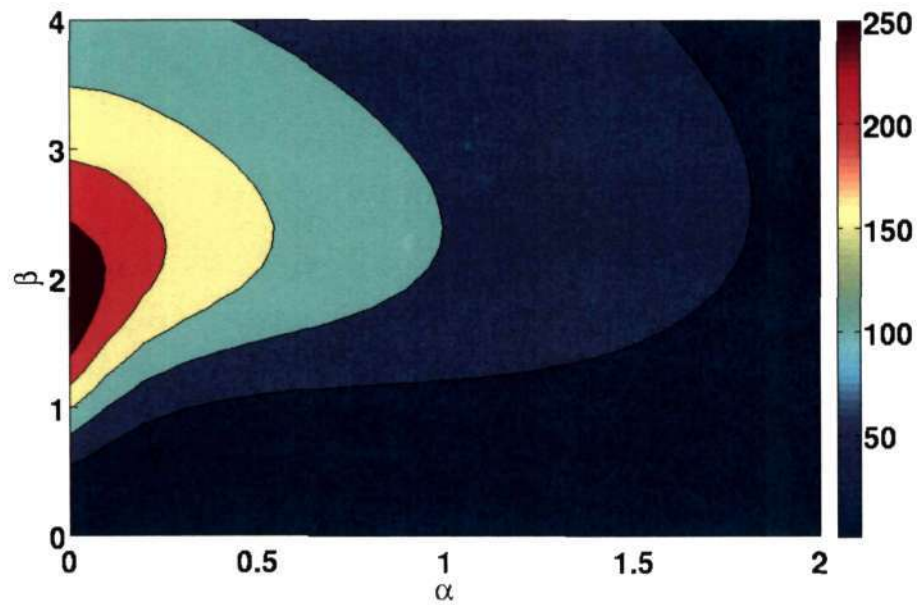


Figure 3.18:  $Gr = -1$ ,  $Pr = 1$ , increasing Prandtl number increases transient growth.

### 3.4.2 Unstable Stratification

The results of unstably stratified Poiseuille flow are similar in nature to that of unstably stratified Couette flow. Unstable stratification causes an increase in transient growth and at high stratification it can lead to instability. At small buoyancy and Prandtl number there is very little change in the  $G_{max}$  contours from the unheated case, this can be seen in Fig 3.17 where  $Gr = -1$  and  $Pr = 0.001$ . Keeping  $Gr$  constant if we increase the Prandtl number to 1 then we can see from Fig 3.18 that there is an increase in the transient growth. The effect of increasing buoyancy is to increase transient growth and also to lead to instability. Keeping the Prandtl number at 0.1 if we increase buoyancy,  $Gr$  to 1000, we see in Fig 3.20 that the transient growth increases.

Figure 3.19:  $Gr = -1, Pr = 10^{-1}$ .Figure 3.20: Same as Fig: 3.19 but  $Gr = -1000$ , increasing Buoyancy increases transient growth.

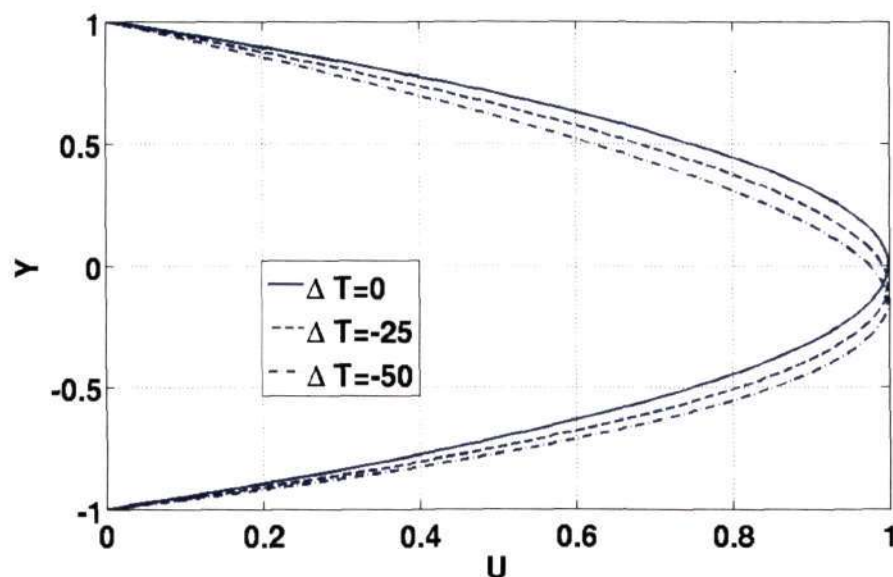


Figure 3.21: Velocity profile for stratified and unstratified case with different level of stratification. The velocity is normalized by the maximum velocity.

### 3.5 Poiseuille Flow: Viscosity and Density Stratification

We have seen that with density stratification there are both qualitative and quantitative changes in the contour of  $G_{max}$  on  $\alpha$ - $\beta$  plane. Thus the next, obvious, question is what effect would viscosity stratification alone and, viscosity and density stratification together have. Variation of viscosity with temperature for small variation in temperature is generally believed to be negligible, but with the Arrhenius model we find that viscosity variation cannot be neglected even for temperature changes as small as  $25^\circ K$ . Eq (3.8) - (3.10) describe the flow with viscosity and density stratification. When we consider a variation of viscosity the mean velocity profile will not be parabolic any more, the profile either has to be computed or derived analytically depending on the model assumed for viscosity.

#### 3.5.1 Mean velocity profile

As in case of Couette flow even here we consider a linear temperature gradient across the channel with the bottom wall at a higher temperature. The profiles

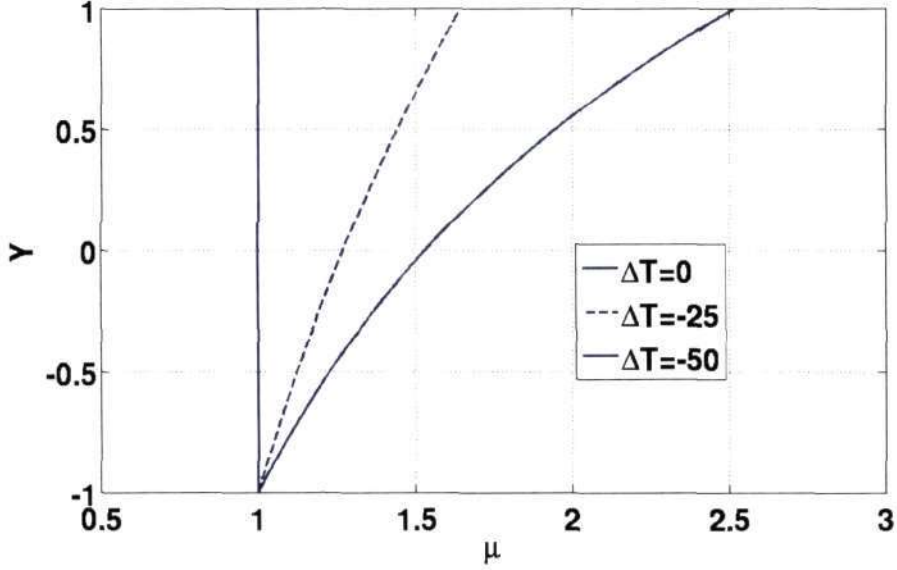


Figure 3.22: Viscosity profile for stratified and unstratified case. The viscosity is normalized by viscosity at the hot wall.

of velocity, viscosity and their derivatives agree well with Sameen(2005) but the profiles are reversed as Sameen considered a linear temperature gradient with the top wall at higher temperature. The linear temperature profile is given by

$$T = \frac{T_H + T_C}{2} - \frac{\Delta T}{2}y \quad (3.34)$$

where  $T_H$  and  $T_C$  correspond to hot and cold wall temperature,  $\Delta T = T_H - T_C$ .

In deriving the stability equation we assumed that the mean flow is only in streamwise direction and varies only along  $y$ , the  $x$  momentum equation for mean flow reduces to

$$\frac{d}{dy} \left( \mu \frac{dU}{dy} \right) = A. \quad (3.35)$$

For an unstratified case we get the parabolic velocity profile  $U = 1 - y^2$ . We consider an Arrhenius model, same as Sameen(2005), described in Eq (3.6). Common liquids like water, alcohol are well described by the model. The viscosity profile for different temperature differences between the two walls in Fig. 3.22. The viscosity is a function of temperature, but temperature is a function of  $y$  thus the mean



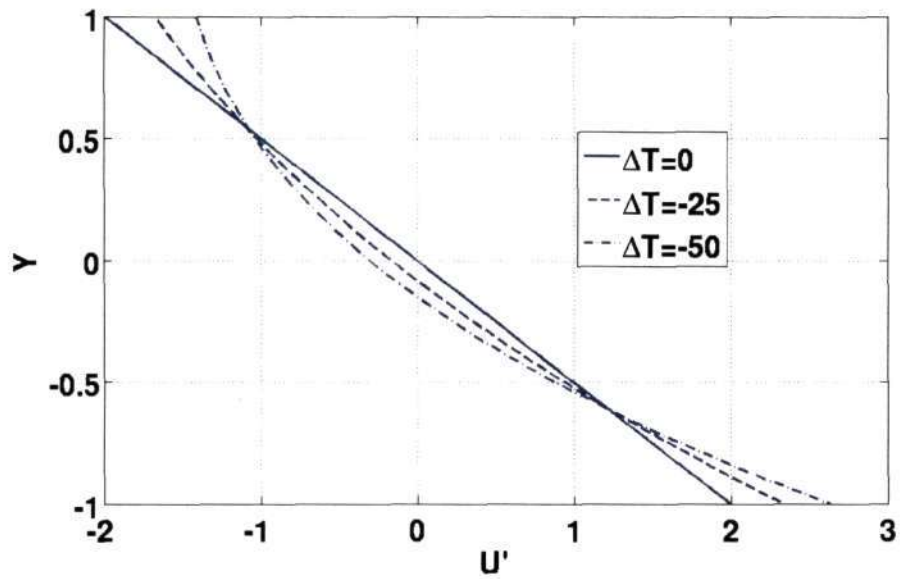


Figure 3.23: Variation of first derivative of velocity with  $y$  for different level of stratification

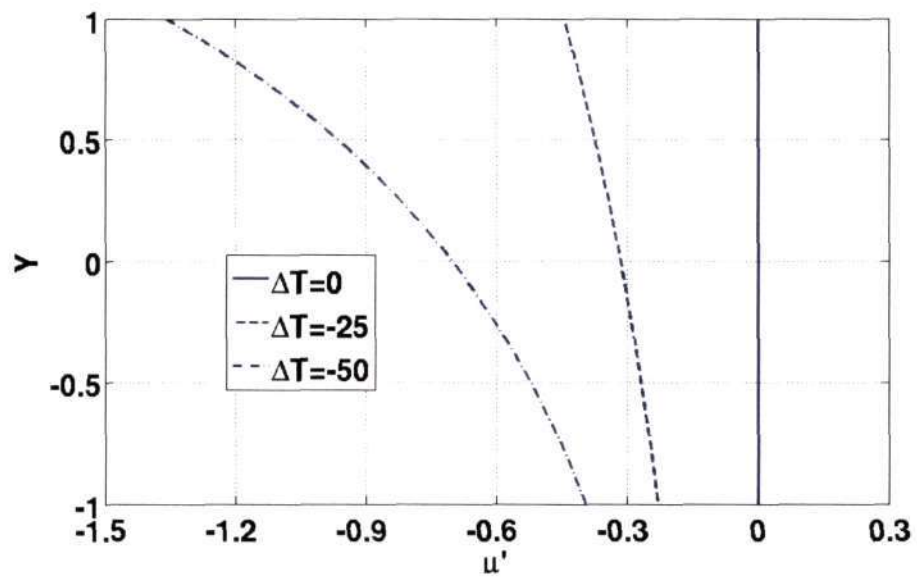


Figure 3.24: Variation of first derivative of viscosity with  $y$  for different level of stratification

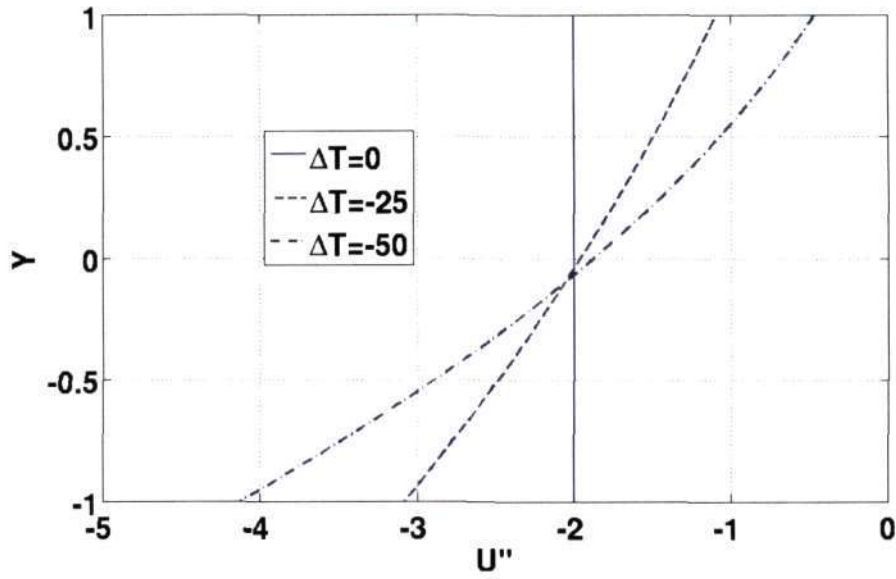


Figure 3.25: Variation of second derivative of velocity with  $y$  for different level of stratification

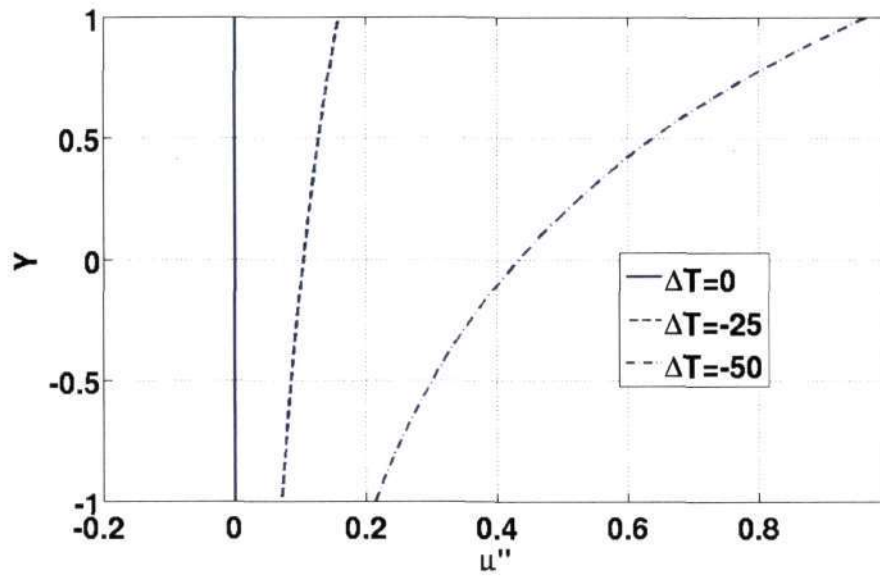


Figure 3.26: Variation of second derivative of viscosity with  $y$  for different level of stratification

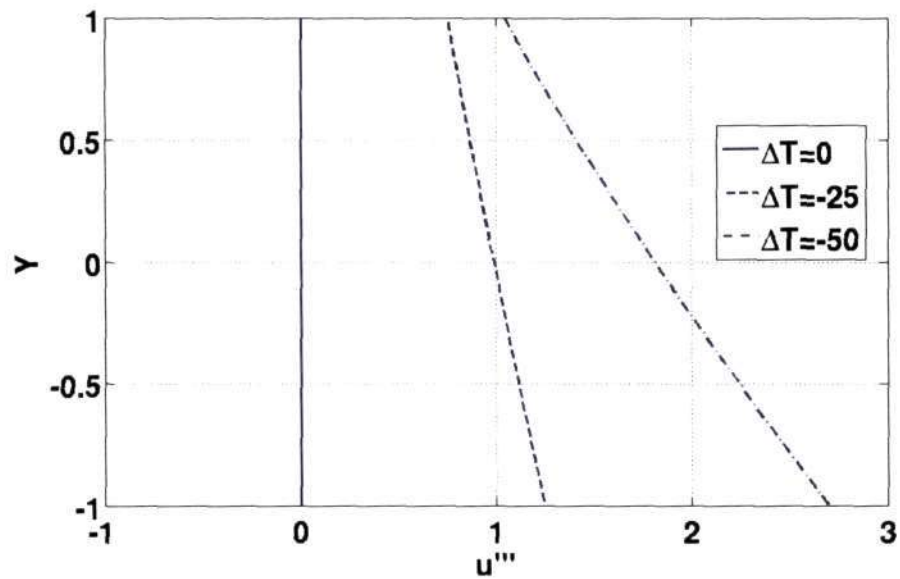


Figure 3.27: Variation of third derivative of velocity with  $y$  for different level of stratification

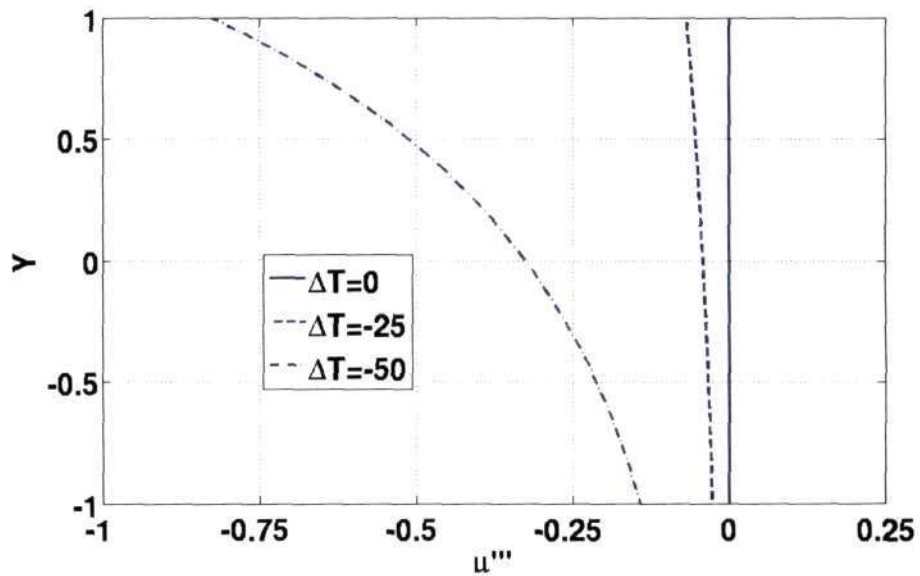


Figure 3.28: Variation of third derivative of viscosity with  $y$  for different level of stratification

viscosity can be expressed explicitly in terms of  $y$ . The first, second and third derivatives of viscosity with respect to  $y$  are shown in Fig. 3.24, 3.26 and 3.28 respectively for different temperature gradients. Integrating Eq (3.35) once we get

$$\frac{dU}{dy} = \frac{Ay}{\nu} + \frac{B}{\nu}. \quad (3.36)$$

As viscosity is not a constant, integrating the above expression depends on how viscosity is defined in terms of  $y$ . For the model we consider, it is not possible to integrate the above equation analytically. We can integrate it numerically to get the velocity profile.

$$U = \int_{-1}^1 \frac{Ay}{\nu} dy + \int_{-1}^1 \frac{B}{\nu} dy + C \quad (3.37)$$

Imposing the boundary condition  $U = 0$  at  $y = \pm 1$  we set  $C = 0$  and numerically integrating the two integrals in Eq (3.37) we can get the other constant,  $B$

$$\frac{B}{A} = - \frac{\int_{-1}^1 \frac{Ay}{\nu} dy}{\int_{-1}^1 \frac{B}{\nu} dy}. \quad (3.38)$$

With  $B$  known, the velocity and its derivatives can be computed numerically, Fig. 3.21 shows the velocity profile for two temperature gradients and the corresponding plots of the derivatives are shown in Fig. 3.23, 3.25 and 3.27. Note that the derivatives of velocity and viscosity appear in the governing equations thus it is necessary to validate their profiles.

### 3.5.2 Viscosity Stratification

We first consider viscosity stratification and neglect gravity effects to study the effect of viscosity stratification alone. At low Prandtl number, 0.0001, there isn't any substantial change, from the unheated case, in the transient growth which can be seen in Fig 3.29. Increasing Prandtl number beyond this value increases the transient growth and the increase is dramatic, there is an order of magnitude change in the transient growth. In Fig 3.30 and 3.31 we can see this dramatic increase in transient growth. The large transient growth seems to be restricted only to

spanwise perturbation waves, for non-zero  $\alpha$  the growth is not as high as for zero  $\alpha$ . Viscosity stratification is far more destabilizing than density stratification.

### 3.5.3 Viscosity and Density Stratification

Including gravity, which brings in the density stratification, causes changes which are expected. When both the stratifications are involved, the effect of viscosity stratification is so large that gravity will not have any effect until  $Gr$  is very large. In the case of stable stratification the gravity does not have any effect up to  $Gr$  of 100, and the effect as we now know, is to reduce the transient growth but the reduction, which is shown in Fig 3.32, is very little. When the Grashof number is increased to 10000 then it has a stabilizing effect reducing the transient growth by an order of magnitude, shown in Fig 3.33 and Fig 3.34. In case of pure density stratification large Grashof numbers resulted in a shift of the region of largest transient growth off the  $\beta$  axis to the right, we don't see such a change when viscosity stratification is included.

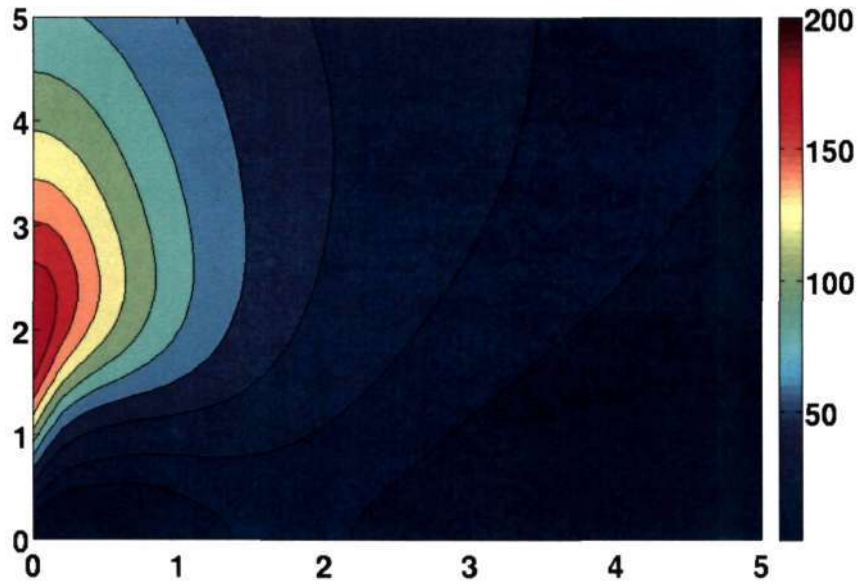


Figure 3.29: Only viscosity stratification,  $Pr = 10^{-4}$

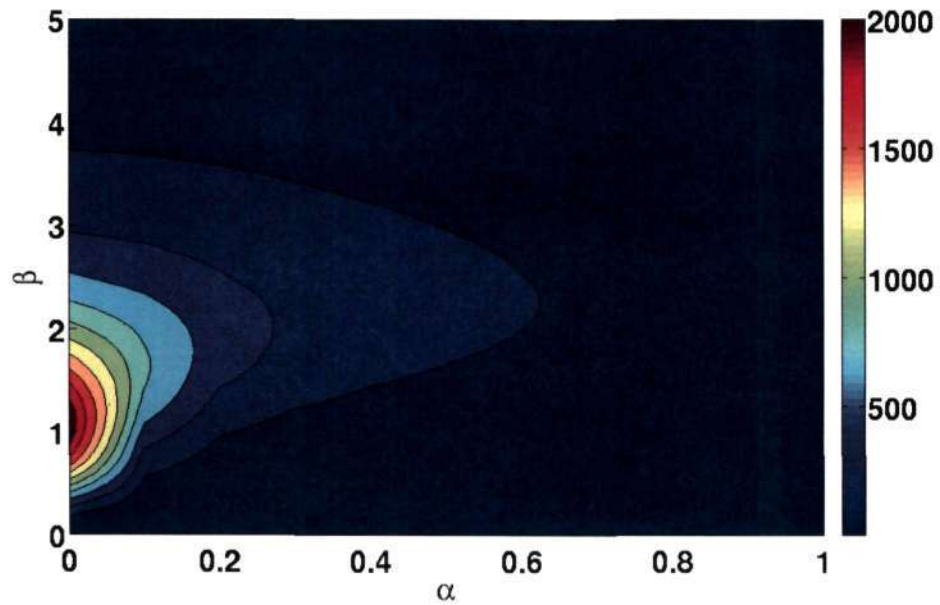


Figure 3.30: increasing  $Pr$  increases the transient growth,  $Pr = 10^{-1}$

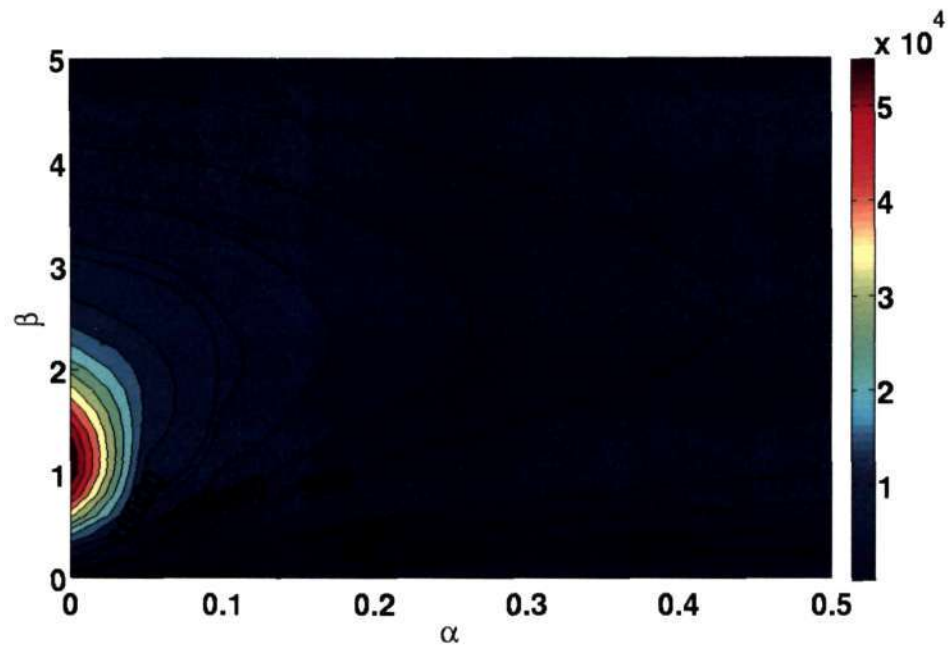


Figure 3.31: There is a dramatic increase in the transient growth,  $Pr = 1$

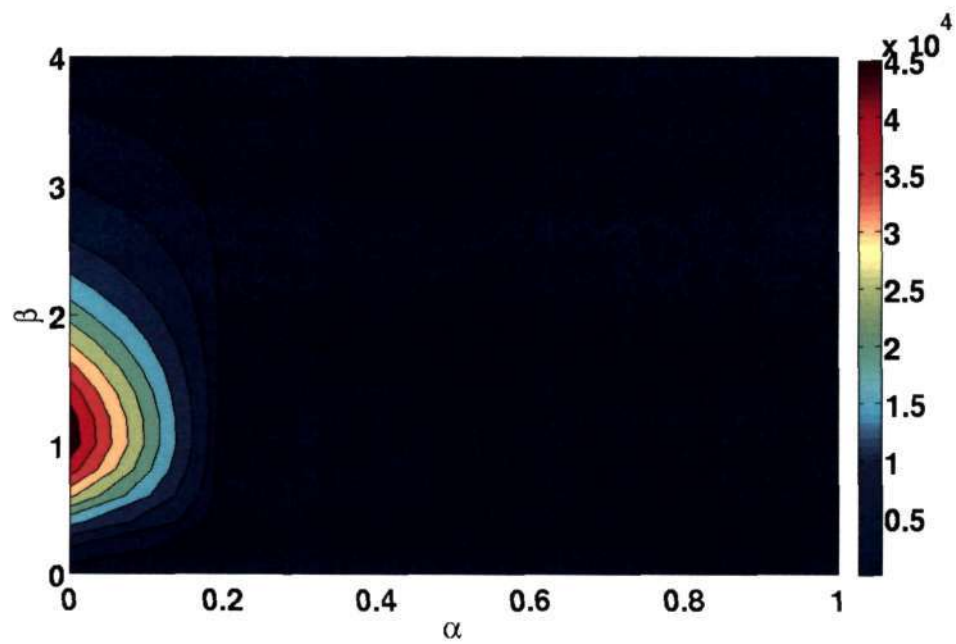
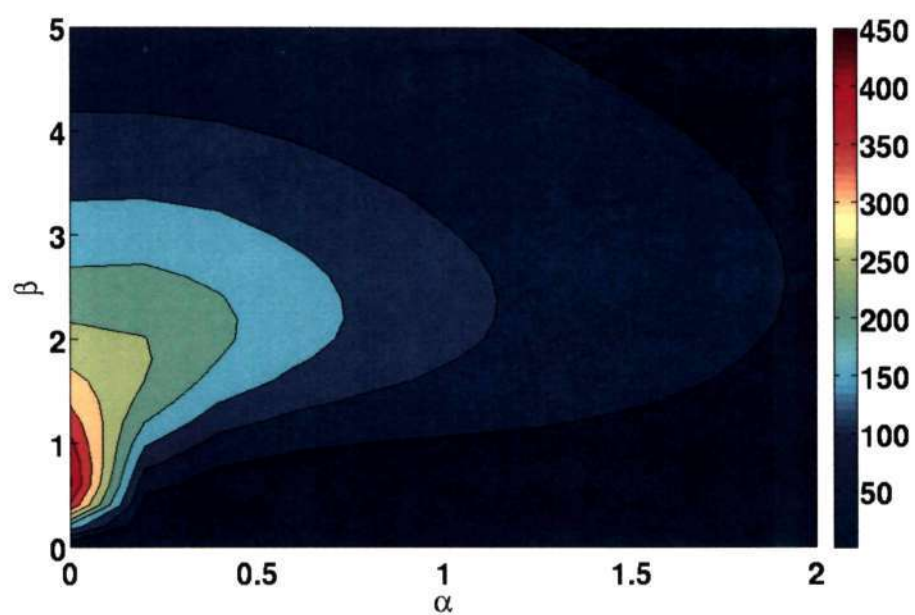
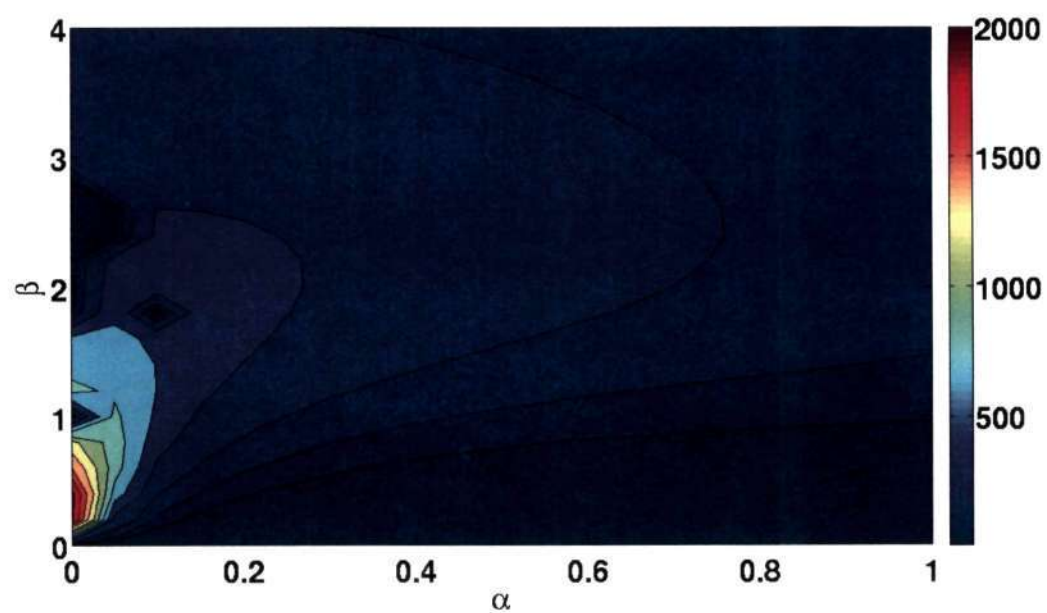


Figure 3.32: Introducing small density stratification suppresses the growth,  $Gr = 100$  and  $Pr = 1$

Figure 3.33:  $Gr = 10000$  and  $Pr = 0.1$ Figure 3.34: At large Grashof the reduction in transient growth is much larger,  $Gr = 10000$  and  $Pr = 1$



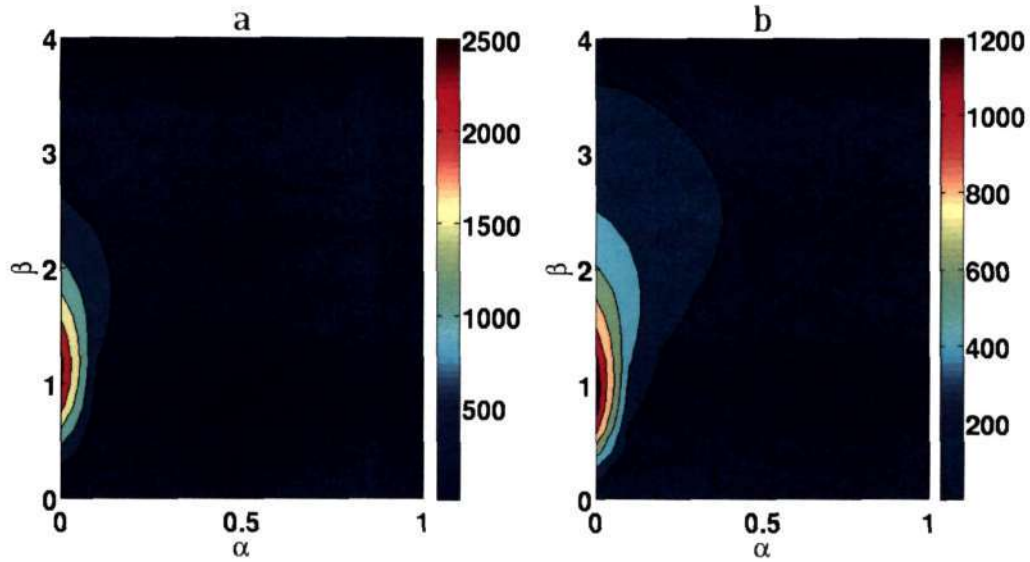


Figure 3.35: Effect of the Choice of  $B$  on the total energy. with  $B = 0.1$  and  $Pr = 0.1$  a)  $Gr = -10000$  b)  $Gr = 1000$

### 3.5.4 Energy Definition

There is no strong physical argument for the choice of  $B$ , thus the choice of  $B$  becomes arbitrary. In all our computations we have chosen  $B$  to be 1. Farrel & Ioannou(1993) argue that changes in the perturbation energy should be related to Reynolds stress in a stratified flow exactly as in an unstratified flow. Based on Farrel and Ioannou's argument the factor turns out to be  $B = Ri/\bar{T}'$ . But if the stratification is in viscosity alone then their argument does not hold as  $Ri$  would be 0, this would imply that potential energy does not contribute to the total energy. Thus we choose a constant factor for  $B$  irrespective of the stratification. It would then be instructive to check how  $B$  will affect the total energy. We choose three values for  $B$ , 0.1, 1 and 10, to study the dependence of total energy on  $B$ . Fig 3.35-3.37 show the growth contours for the three values of  $B$  0.1, 1, 10 respectively. The contours are plotted for  $Pr=0.1$ ,  $Gr=-1000$  and  $Gr=1000$  for (a) and (b) of each figure respectively. The nature of change in both a and b are similar but there is very little change. There is hardly any change when between  $B=0.1$  and  $B=1$  case, there is a slight change in the contour when  $B$  is changed to 10 but it does not affect the maximum growth. There is an increase in the growth of regions away from the region of maximum growth but the increase is slight. Thus for any choice

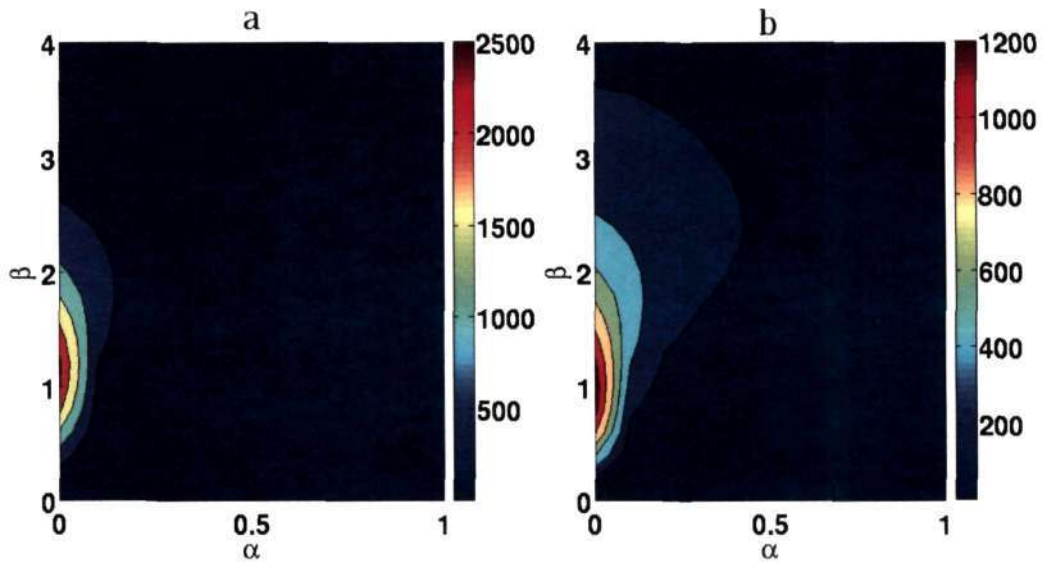
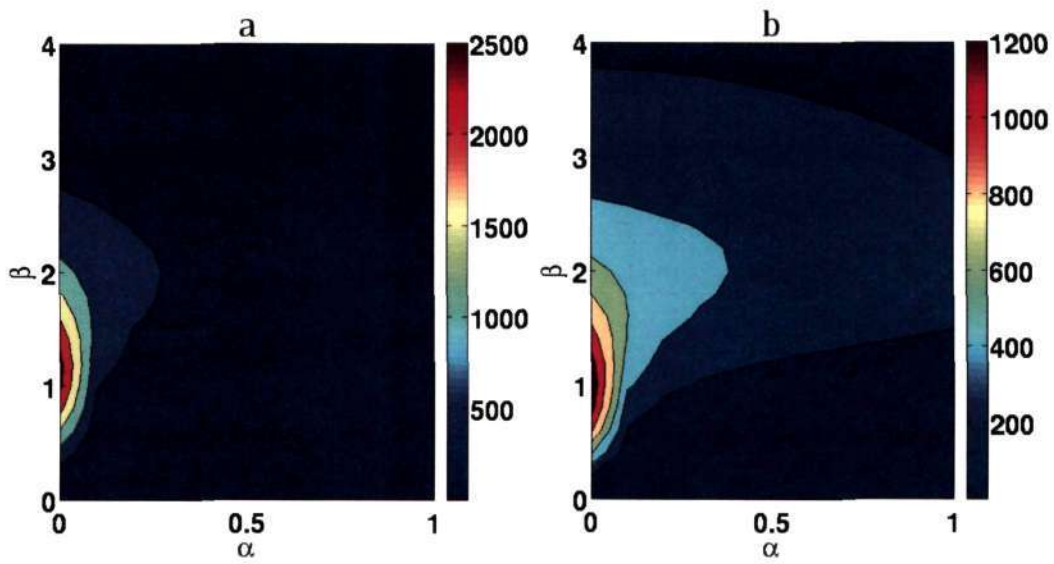


Figure 3.36: Same as Fig 3.35,  $B = 1$

of  $B$  within upper and lower limit of  $B$  chosen the results obtained are consistent. But if  $B$  is very large or very small then the solutions might change.

Figure 3.37: Same as Fig 3.35,  $B = 10$



## CHAPTER 4

# CONCLUSIONS AND FUTURE OUTLOOK

The aim of our work is to study the effect of stratification, in density and viscosity, on the short time stability of shear flows. We study both the inviscid and the viscous problems.

We start with the inviscid analysis of a stable density stratification in Couette flow. Earlier work on bounded stratified shear flow concentrated on the long time behavior of the system, no attempt was made to study short time dynamics until Farrel & Ioannou in 1993 who study it numerically. We have tried to study the problem analytically in the inviscid case. The toy model by Brown & Stewartson (1980) for unbounded Couette flow has been adapted to bounded Couette flow. We find that there is an unbounded growth for a singular initial perturbation in temperature and a  $1/t$  algebraic decay for a smooth initial perturbation same as Brown & Stewartson (1980). We probe into the short time dynamics of this to model and show that there indeed can be a transient algebraic growth for Gaussian initial thermal perturbations.

There is an unbounded sublinear growth,  $t^{1/2-n}$ , in the full inviscid problem for singular initial thermal perturbations, but a  $t^{-3/2+n}$  algebraic decay for any smooth initial condition at large times. We make heuristic arguments for the full inviscid problem that as we make a transition from singular to smooth initial thermal perturbation there will be an initial growth in stream function and energy before the asymptotic decay. As future aspect of the full inviscid problem, it has to be verified and validated by numerical integration of the contour integral.

In the viscous problem we study density and viscosity stratification, for stable as well as unstable stratification, in Couette and Poiseuille flow. Some of the results are expected but some results are unexpected and new. In case of stable density stratification in Couette and Poiseuille flow there is a suppression of transient growth as one would have expected. The modes that caused the dominant transient growth in the unstratified case are different from the stratified case, e.g. the streamwise rolls caused the maximum amplification in unstratified case but these rolls are no longer streamwise but have a slight tilt in the spanwise direction when there is stratification, which we believe is an unexpected result. The

physical mechanism for this phenomenon has to be looked into, perhaps through Direct Numerical Simulations (DNS). In the case of unstable density stratification in Couette and Poiseuille there is an enhancement of the transient growth but unlike in stable stratification there is no change in the modes causing the maximum transient growth.

When we consider viscosity stratification we get the most dramatic results. In the case of pure viscosity stratification there is a dramatic increase in the transient growth, but no change in the modes causing the maximum amplification. On including stable density stratification we do not see a substantial change in the transient growth, except for a very slight quantitative decrease. There is no qualitative change in the nature of transient growth unlike in the case of pure density stratification. —————

## References

- [1] BAKAS, N., IOANNOU, P. & KEFALIAKOS, G. 2001 The emergence of coherent structures in stratified shear flow. *J. Atmos. Sci.* 58, 2790-2806.
- [2] BANKS, W., DRAZIN, P. & ZATURSKA, M. 1976 On the normal modes of parallel flow of inviscid stratified fluid. *J. Fluid Mech.* 75, 149-171.
- [3] BOOKER, R. & BRETHERTON, P. 1967 The Critical layer for internal gravity waves in a shear flow. *J. Fluid Mech.* 27, 513-539.
- [4] BIAU, D. & BOTTARO, A. 2004 The effect of stable thermal stratification on shear flow instability. *Phys. Fluids* 16(14), 4742-4745.
- [5] BROWN, S. & STEWARTSON, K. 1980 On the algebraic decay of disturbances in a stratified linear shear flow, *J. Fluid Mech.* 100(4), 811-816.
- [6] BUTLER, K. M. & FARREL, B. F. 1992 Three-dimensional optimal perturbations in viscous shear flow. *Phys. Fluids* 4(8), 1637-1650.
- [7] CASE, K., M. 1960a Stability of inviscid plane Couette flow. *Phys. Fluids* 3(2), 143-148.
- [8] CASE, K., M. 1960b Stability of idealized atmosphere. I. Discussion of results. *Phys. Fluids* 3(2), 149-154.
- [9] CHIMONAS, G. 1979 Algebraic disturbances in stratified shear flows. *J. Fluid Mech* 90, 119.
- [10] DIKII, L., A. 1960 On The Stability Of Plane Parallel Flows Of An Inhomogeneous Fluid. *Dokl. Akad. Nauk* 24, 249-257
- [11] ELIASSEN, A., HOILAND, E. & RIIS, E. 1953 Two-dimensional perturbation of flow with constant shear of a stratified fluid. *Institute of weather and climate research, Norwegian Academy of Sciences and Letters* 1, 1-28.
- [12] ELINGSON, T. & PALM, E. 1975 Stability of linear flows. *Phys. Fluids* 18, 487-488.

- [13] FARRELL, B. & IOANNOU, P. 1993 Transient development of perturbations in stratified shear flow. *J. Atmos. Sci.* 50, 2201-2214.
- [14] FARRELL, B. & IOANNOU, P. 1996 Generalized stability theory. part 1 : Autonomous operators. *J. Atmos. Sci.* 53, 2025-2040.
- [15] FARRELL, B. F. 1988 Optimal excitation of perturbations in viscous shear flow. *Phys. Fluids* 31, 2093-2102.
- [16] KUO, H. L. 1963 Perturbations of plane Couette flow in stratified fluid and origin of cloud streets. *Phys. Fluids* 6(2), 195-211
- [17] KOU SHIK, S. 2007 *Direct numerical simulation of transition in unstably stratified Poiseuille flow*, Masters Thesis, Engineering Mechanics Unit, Jawaharlal Nehru Center for Advanced Scientific Research.
- [18] LANDAHL, M. T. 1980 A note on an algebraic instability of inviscid parallel shear flows. *J. Fluid Mech* 98(2), 243-251.
- [19] ORR, W. M. 1907 The stability or instability of the steady motions of a perfect liquid and of viscous liquid. *Proc. Roy. Irish Acad. A* 27, 91-138.
- [20] PEDLOSKY, J. 1987 *Geophysical fluid dynamics*, Springer.
- [21] REDDY, S. C. & HENNINGSON, D. S. 1993 Energy growth in viscous channel flows. *J. Fluid Mech* 252, 209-238.
- [22] SAMEEN, A. 2004 *Stability of Plane Channel Flow with viscosity stratification*. PhD Thesis, Department of Aerospace Engineering, Indian Institute of Science.
- [23] SAMEEN, A. & GOVINDARAJAN, R. 2007 The effect of wall heating on instability of channel flow. *J. Fluid Mech.* 577, 417-442.
- [24] SCHMID, P. J. & HENNINGSON, D. S. 2001 *Stability and Transition in Shear Flows*. Springer-Verlag, New York.
- [25] TREFETHEN, L. N. & EMBREE, M. 2005 *Spectra and Pseudospectra: The behavior of nonnormal matrices and operators*, Princeton University Press, New Jersey
- [26] TREFETHEN, L. N., TREFETHEN, A. E., REDDY, S. C. & DRISCOLL, T. A. 1993 Hydrodynamic stability without eigenvalues. *Science* 261, 578-584.